Familiarity-induced differential activation and connectivity patterns in the language network

Muskaan Verma

Supervisor: Dr Arpan Banerjee

Cognitive Brain Dynamics Lab
National Brain Research Centre

A dissertation submitted in partial fulfilment of the requirements for the award of the
Master's in Neuroscience

May 2022

I would like to dedicate this thesis to my loving parents ...

Declaration

I, Muskaan Verma hereby declare that the work presented in the form of the dissertation titled "Familiarity-induced differential activation and connectivity patterns in the language network" was carried out by me under the guidance of **Dr Arpan Banerjee** at National Brain Research Centre (Deemed to be University), Manesar, Haryana, India.

I declare that no part of the dissertation contains any plagiarised material. Any previously published or other material sourced from anywhere else has been appropriately attributed to the source.

I also declare that no part of this dissertation has been previously submitted for the award of any degree or diploma to National Brain Research Centre (Deemed to be University) or to any other university.

Muskaan Verma
May 2022

Acknowledgements

Foremost, I would like to express my heartfelt gratitude to my research supervisor, Dr Arpan Banerjee, Scientist V, National Brain Research Center, for permitting me to pursue the research question of my interest. His timely, informed advice and meticulous scientific scrutiny enhanced my analytical abilities immensely, and this work would not have been complete without his contributions.

I profusely thank my mother, who helped shape this young woman and for her vehement faith and support in my constant pursuit of awe and wonder. Her ability to provide a bird's eye perspective has helped me solve many problems, both personal and professional, and her upbeat attitude and optimism has helped propel me forward towards my ambitions.

This thesis is a product of numerous thought provoking discussions and troubleshooting sessions with my seniors. I thank Shyamchand, Azman, Anagh, Anshika, Nisha, Gargi, Neeraj, Yudhajit and Kirti for being remarkably even-tempered and collaborative.

I also thank my friends Nitish, Lakshay, Bharat and my brother, Yash for providing the necessary technical (and non-technical) guidance.

Abstract

How do the students comprehend the scientific texts from various domains with varying levels of background knowledge? This study aims to look at the differences in the BOLD response while scientific reading across L1 participants with high and low familiarity with the expository text during a fixation-related naturalistic fMRI reading paradigm in the language-related areas of the brain. This data is the first in its kind, combining multiband acquisition (with 0.4 seconds of repetition time) and the expository text "reading in the wild" experiment in the MRI scanner, complemented by the eye-tracker. Our analysis integrated the inference from the activity and the connectivity in the left hemispheric language-specific regions parcellated functionally (sentence > non-words). Our results revealed a non-linear trajectory in the activations and the functional connectivity with increasing familiarity (measured on a Likert scale of 1-5), with its maxima at familiarity two and decreasing overall. We also submit that the higher inter-hemispheric connectivity while comprehending a text with less background knowledge and more increased intra-hemispheric connectivity while reading a much familiar text. Also, though the left angular gyrus was consistently shown in the language comprehension task in the literature, but it had a negative percent signal change and seemed to follow the activity profile trend of right hemispheric regions, indicating its role in the saliency network, which tends to be right-lateralized. The causal mechanism of the right and left hemispheric language network, along with the integration of other brain networks, is still under scrutiny.

Table of contents

List of figures

List of tables

Nomenclature

Acronyms / Abbreviations

AF Acceleration factor

BIDS Brain Imaging Data Structure

BOLD Blood Oxygenation Level Dependent

CONN Connectivity Toolbox

EEG Electroencephalogram

EPI Echo-planar imaging

FDR False Discovery Rate

fMRI Functional Magnetic Resonance Imaging

FNC Functional Network Connectivity

FOV Field of view

FWE Family-wise Error

GLM General Linear Model

GRAPPA GeneRalized Autocalibrating Partial Parallel Acquisition

HRF Hemodynamic Response Function

HySCo Hyper-elastic Susceptibility Artifact Correction

LAngG Left angular gyrus

LAntTemp Left anterior temporal cortex

LIFG Left inferior frontal gyrus

LIFGorb Orbital part of left inferior frontal gyrus

LMFG Left middle frontal gyrus

LPostTemp Left posterior temporal cortex

MEG Magnetoencephalography

MPRAGE Magnetization Prepared - RApid Gradient Echo

MR Magnetic Resonance

MTG Middle Temporal Gyrus

RAngG Right angular gyrus

RAntTemp Right anterior temporal cortex

RBQ Reading background questionnaire

RIFG Right inferior frontal gyrus

RIFGorb Orbital part of right inferior frontal gyrus

RMFG Right middle frontal gyrus

ROI Region of Interest

RPostTemp Right posterior temporal cortex

RSVP Rapid Serial Visual Presentation

SPM Statistical Parametric Mapping

STEM Science, technology, engineering and mathematics

STG Superior Temporal Gyrus

TE Echo time

TR Repetition Time

Chapter 1

Introduction

1.1 Functional Magnetic Resonance Imaging and BOLD response

Functional imaging was introduced to already existing MRI techniques in 1992 to measure spatially specific brain activity. After that, the number of fMRI publications rapidly increased, exploring the different cognitive phenomenons, corresponding neural activity and connectivity among different brain regions. The certitude of the localized blood flow contributes to the "functional" of the fMRI and is nothing less than a gift to cognitive neuroscience. The fact that local cerebral blood oxygenation level proportionally changes with transient neuronal activity in the brain region, known as neurovascular coupling, is utilized to study BOLD (blood oxygenation level-dependent) contrasts. The magnitude of the BOLD is studied as the surrogate for neuronal activity. Researchers have theorized the phenomenon as the increase in energy demands as a neuronal population is activated, resulting in increased blood flow. The local influx of oxygenated blood results in a higher oxy-/deoxy-hemoglobin ratio, reflecting an increased MRI signal, in contrast with the surrounding tissue, mapped statistically onto the anatomical image, refer to figure 1.1.

The BOLD response canonically rises and falls under a particular trajectory known as hemodynamic response function (HRF), with an initial dip followed by a slower, higher amplitude peak and the following longer undershoot. Peak response appears after 4-6 seconds after the stimulus onset and returns to baseline approximately after 12 seconds as given in the figure 1.2. HRF is modeled in most software by a double gamma function. In order to correctly extract the activity relating to a specific

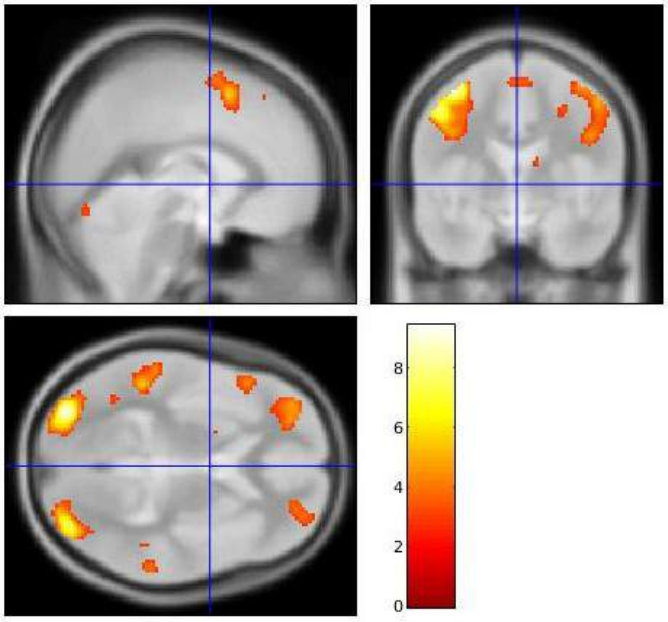

Fig. 1.1 fMRI t-map overlaid on anatomical image with color of every voxel representing the T-value for a given contrast

task, one should take task design, artifact removal and correct statistical analysis into consideration.

1.2 Advancements: Fast fMRI

With the ever-advancing MR technology, we can now capture fMRI data at a much faster rate. This short TR (high sampling rate) data enables the study of more rapid neural dynamics but also adds to the problem of increased temporal noise. Earlier believed that the noise follows a much faster dynamics than the BOLD response; hence, band passing specific frequencies were accepted as the best-suited filtering process. To capture fast neural oscillations, excluding the faster data bandwidth can significantly lose signal. Recently people have argued that faster acquisition, along with additional artifacts removal can help us detect the neural response of higher frequencies, with some challenges preordained. The fMRI is increasingly fine-tuned for spatial specificity and can capture fine-scale architecture, for, say, cerebral cortical columns. Still, there is a constant trade-off between fMRI's spatial and temporal resolutions, refer to figure 1.3. The images get blurrier with the increasing temporal resolution, reducing brain coverage. But, parallel imaging technologies, also known as simultaneous slice acquisition, have enabled the acquisition of whole-brain functional images at sub-second repetition

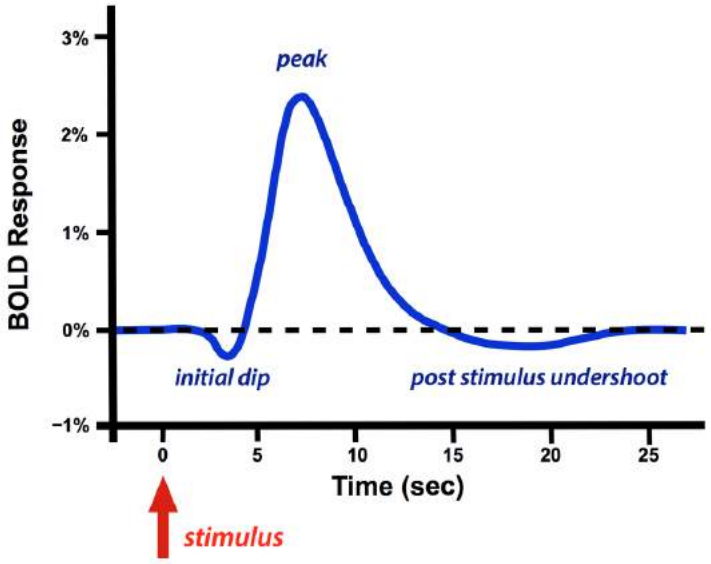

Fig. 1.2 The rise and fall of canonical Hemodynamic Response Function peaking at 6-8 second, credits : MRI questions

time.

Current non-invasive neuroimaging methods include EEG, fMRI and MEG. Both EEG and MEG can capture higher neural oscillations but cannot precisely localize the activation source. On the other hand, fMRI is known to be spatially precise, but it has a low temporal resolution as it indirectly captures neural activity by measuring vascular responses. With recent advancements, fast fMRI has been shown to detect frequencies of even up to 0.75 Hz, compared to the earlier limit of 0.1 Hz, expanding our frequency scale under-inspection (Polimeni and Lewis, 2021).

Studies have also proven that the BOLD response becomes faster with rapidly changing stimuli. The ability to capture faster neural oscillation with comparatively high spatial resolution can provide insights for higher cognitive processing during naturalistic settings. Moreover, this challenges the assumption the BOLD response is "sluggish" and has a lag of 4-6 seconds after the stimulus onset, it can also shed light on the ongoing debate of HRF being or not a representative of direct neuronal activity. And maybe the TR not the HRF is the rate-limiting factor for detecting the BOLD response.

Attempts of increasing the sampling rate come with even more sources of errors and higher noise. Foremost, the basis function comes into an interrogation as the canonical HRF function may not correctly reflect the fast dynamics; also, one must upgrade the

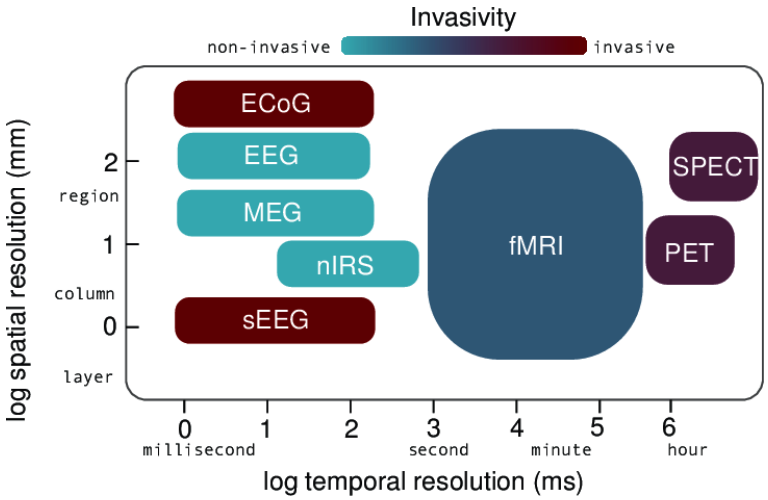

Fig. 1.3 Spatial and temporal resolution of different neuroimaging modalities (Pedregosa-Izquierdo, 2015)

study designs to exploit the high temporal specificity of the HRF. Some changes were also made during the preprocessing pipeline and analysis to combat the noise due to fast sampling rate, see methods section for further details.

Some changes were also made during the preprocessing pipeline and analysis to combat the noise due to fast sampling rate, see methods section for further details.

1.3 Background and Objective

1.3.1 Hypotheses

We aim to find the bio-markers, currently limited only to the language parcels, of the level of expertise in a subject. What changes in the regions responsible for sentence processing when one reads a passage from a scientific domain they know very well compared with processing a passage about which they understand nothing?

How is this study different? The predictability of the immediate next word and the predictability of the entire topic are two different cognitive phenomenons, but related, the latter one being more global. We have called it "contextual familiarity" and aim our analysis to determine the different activation patterns between "non-experts" and "experts", colloquially put.

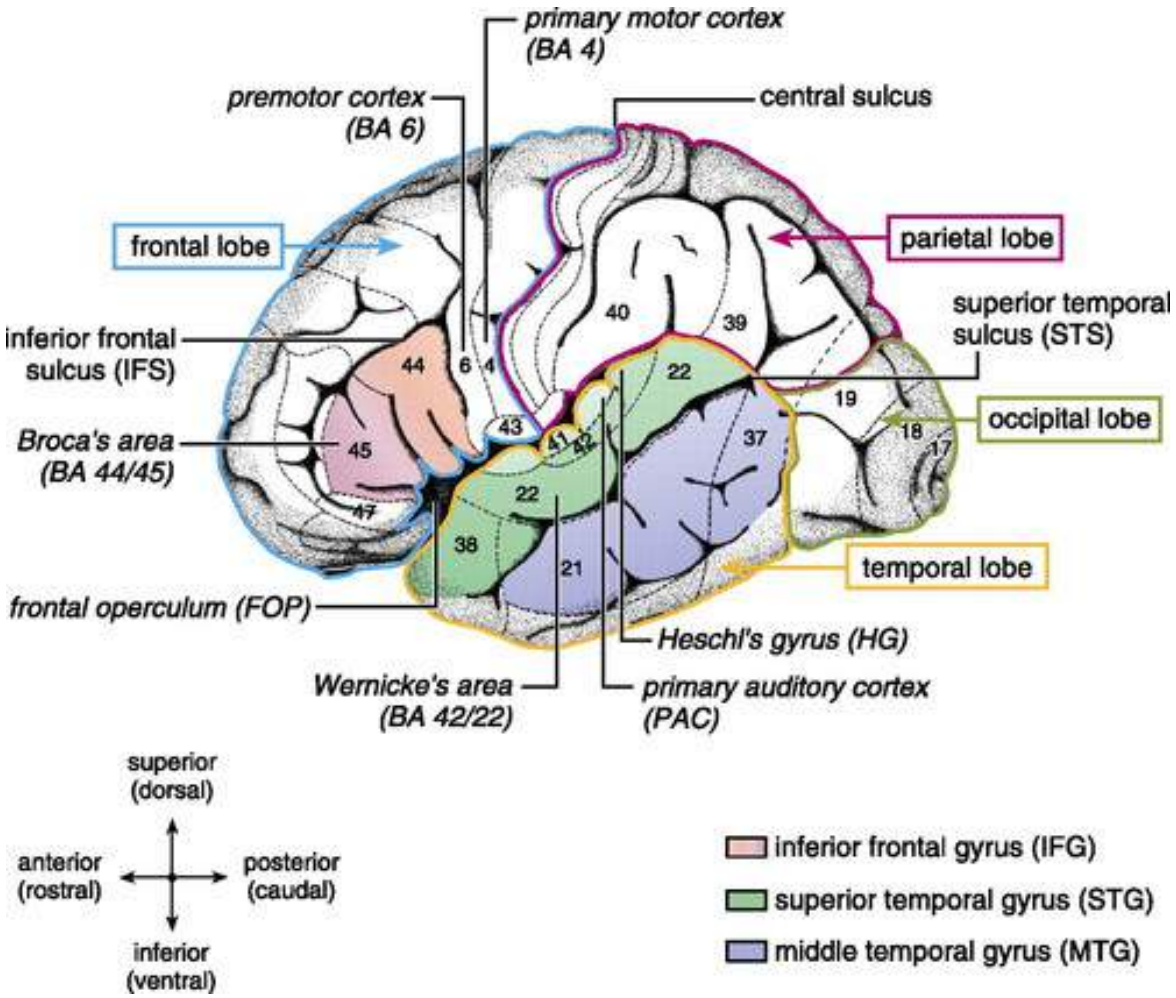

Fig. 1.4 The reading brain: All the areas reported previously, responsible for language perception and processing through both audio and visual modalities

1.3.2 The Reading Brain

The Language network is left-lateralized, mainly comprising the left inferior frontal gyrus, Broca's area, and the superior-middle part of the posterior temporal gyrus, Wernicke's area. Additionally, the activation of some regions from the "extended network" was also reported to light up during sentence comprehension. Refer to the table 1.5 for all the core language areas along with their tentative functions(Hertrich et al., 2020). Comprehending a text starts with processing the visual information in the visual word form area (VWFA), also known as the brain's letterbox, activated for orthographic symbols, including letters and words. The area is known to have an integrating role in language and attention (Chen et al., 2019). These words are then grouped into graphemes and mapped to phonemes by the left angular gyrus. Syntactic

processing takes place in inferior frontal and superior temporal brain regions. The middle temporal gyrus (MTG) and the superior temporal gyrus (STG) are responsible for translating speech sounds to word meanings.

Semantic information is distributed over the temporal gyri, the left middle and inferior parts. The frontal areas, namely the left inferior frontal gyrus, are recruited to integrate phonological, lexical-semantic, and syntactic information. There lies a temporal hierarchical structure from visual input to final integration and sentence processing, recruiting different areas moving from posterior to anterior.
Refer to figure 1.4 for the illustration depicting the language areas of the brain (Tripathi et al., 2020).

1.3.3 Literature Survey

The phenomenon that familiarity with the stimulus leads to attenuated neural responses is well-established in the literature as 'familiarity suppression', observing sharper neural tuning and sparser population representation for familiar stimuli. On top of that, a recent study has shown that in the visual system, neural responses truncate faster in addition to decreased amplitude in response to selecting a target image embedded in a familiar distractor vs the novel ones, hence neurons returning to the state of readiness more quickly, reason proposed. Moreover, after studying word co-occurrence probability and context-free grammar surprisal, researchers concluded that language-specific circuits implement linguistic predictive coding instead of previously argued domain-general, multi-demand network. Researchers from MIT and Meta AI independently concluded that the deep learning models capable of predicting the next word successfully classified also the neuroimaging data acquired while performing the next word prediction task.
Familiarity: A group of researchers studied the comprehension under the fMRI of simpler, familiar texts with complex, more domain-specific texts. They uncovered global coherence, that is, the activation of the extended language network while processing familiar texts. The dorsomedial prefrontal cortex and the bilateral anterior temporal lobe were reported to process inference making. On the contrary, local coherence was registered during more complex texts. The prominent areas were the dorsolateral and ventrolateral prefrontal cortex, the left inferior frontal gyrus and the left inferior and posterior parietal lobe. Inferring that the semantic complexity of the paragraph changes the contribution from different processing units.
Scientific (Expository) Texts: Type of information acquisition while reading can be grouped into two genres: narratives (stories) and exposition (essays). Comprehending these two types of texts involves slightly different mental resources and at varying

degrees due to their different structure and content (Mar et al., 2021). Narrative texts are stories chronologically following a particular structure, revolving around a theme and plot. They have a much easier and more familiar order of content. Expository texts inform ideas about a specific topic containing definitions, explanations, descriptions and arguments. Since they have a more complex structure and weave intricate thoughts, they were argued to be more demanding in comprehension and later recall than stories. We wanted to understand the basis of global conceptual familiarity; hence, we limited the study to expository texts. It is easier to have a self-reported score for familiarity with a science domain than a story line that requires significantly less prior knowledge to understand completely. Expository texts need substantial prior knowledge, and readers with strong domain-specific understanding are believed to infer concepts from the same domain much more efficiently. On the other hand, low prior knowledge leads to difficulty comprehending low cohesion prevalent in many scientific texts adding to the inadequacy in generating inferences across ideas. Hence, scientific text comprehension relies heavily on domain-specific knowledge and the ability to integrate the information from previously read multiple sources.

1.4 Objective

The current cognitive neuroscience study investigates how sentence processing in the language-specific regions varies as the function of contextual familiarity while the participants read expository texts in a naturalistic fixation-related-fMRI paradigm. We aim to look at:

1. **How does the activation pattern changes in the language-specific regions while comprehending scientific sentences with increasing contextual familiarity with the subject of the paragraph?**

2. **How does the functional connectivity changes in the language network while comprehending scientific sentences with increasing contextual familiarity with the subject of the paragraph?**

	Brain structure	Language-related function	Functional network	Connectivity
1	Auditory cortex (A1)	Speech perception, monitoring	Auditory system	Subcortical afferents, ventral and dorsal stream, cross-modal connectivity
2	STG anterior to A1	Representation of auditory word forms	Auditory system, lexical pathway	Ventral auditory stream, connectivity to the semantic system
3a	Posterior part of the frontal language areas (BA44)	Speech generation	Phonological network	Dorsal language pathways, frontal aslant tract
3b	Posterior STG, planum temporale	Representation of phonological units, speaker adaptation	Auditory-phonological network	Dorsal language pathways
3c	Temporal-parietal boundary and part of SMG	Speech repetition, phonological-sensorimotor interface	Sensorimotor-auditory network	Dorsal language pathways
3d	Dorsal premotor cortex	Speech preparation and repetition	Motor system	Auditory-motor connectivity
4a	Middle part of the frontal language areas (BA44, 45)	Sentence generation	Syntactic network	Dorsal and ventral frototemporal language pathways, frontal aslant tract
4b	Posterior Parts of STG, STS, and MTG	Sentence processing	Syntactic network	Dorsal and ventral frontotemporal language pathways
5a	Anterior part of the frontal language areas (BA45)	Semantic processing	Lexical-semantic network	Ventral language pathways
5b	Anterior and posterior parts of STS and STG	Semantic processing	Lexical-semantic network	Ventral language pathways, longitudinal tracts within the temporal lobe

*The numbers and letters in the first column correspond to the numbers in **Figure 1**. A1, primary auditory cortex; BA, Brodmann area; MTG, middle temporal gyrus; SMA, supplementary motor area; SMG, supramarginal gyrus; STG, superior temporal gyrus; STS, Superior temporal sulcus; IFG, Inferior frontal gyrus.*

Fig. 1.5 Tentative functions and connections of the "core language areas"

	Brain structure	Language-related function	Functional network	Connectivity
6a	Sensorimotor cortex	Motor embodiment of language: somatotopic aspects of articulation and body-related semantics	Motor system	Posterior IFG, Premotor cortex, SMA, and widespread connectivity to the semantic system
6b	SMA and pre-SMA	Cognitive control: initiation and inhibition after error detection	Motor system, multiple demand system	Frontal aslant tract (to motor and premotor cortex and IFG) and widespread input via subcortical pathways
6c	Dorsolateral prefrontal cortex	Cognitive-attentional-executive control: language switching, task switching, management of non-literal meanings	Multiple demand system	Fronto-parietal-occipital pathways, various targets in frontal cortex, task-specific connectivity between the multi-demand system and various memory systems
6d	Orbitofrontal cortex	Semantic emotion and valence processing	Social-emotional processing network	Uncinate fasciculus toward the temporal lobe, connectivity to the limbic system, and the default mode system
6e	Temporal pole	Representation of emotional words	Semantic system, social-emotional processing network	Uncinate fasciculus toward the frontal lobe,
6f	Inferior parts of the temporal lobe	Visual speech, reading, visual and supra-modal mental objects that are linked to word forms	Semantic system	Longitudinal tracts within the temporal lobe, cross-modal connectivity
6g	Angular gyrus, temporo-parietal junction	Pragmatic processing, context integration, words with multiple meanings, perspective taking, social cognition	Default mode network, theory of mind network, semantic network	Longitudinal tracts within the temporal lobe, multi-modal connectivity, connectivity to medial prefrontal and cingulate cortex

Most of these language-related functions are more or less lateralized to the left hemisphere.
*The first column indicates the respective regions depicted in **Figure 1**. SMA, supplementary motor area; IFG, Inferior frontal gyrus.*

Fig. 1.6 Tentative functions and connectivity of "margin" language areas

Chapter 2

Methods and Materials

2.1 Neuroimaging data

The data for the current study is taken from BIDS validating, open-source neuroimaging data platform: OpenNeuro, submitted by Friederike Seyfried on 2019-10-21. The data was collected at Pennsylvania State University, U.S.A. and Brain, Language, and Computation Lab, Hong Kong and used in the previous study (Hsu et al., 2019) (Li et al., 2022).

Acquisition Parameters

1. **MRI Data Acquisition**
   Data were acquired using a 3T Siemens Magnetom Prisma Fit scanner with a 64-channel phased-array coil at Pennsylvania State University Hershey Medical Center in Hershey, Pennsylvania.

   (a) **T1-Weighted Structural Images**
   A six-minute MPRAGE scan with T1-weighted contrast acquiring anatomical image was done with a blank screen, and the participants were informed that they could close their eyes. Parameters for acquiring the anatomical images were as follows:

   (b) **Resting-state MRI Data**
   Five minutes of resting-state echo planar image was completed while participants stared at the cross in the center of the screen and thought about

Parameter	Value
Number of Slices	176
Slice Acquisition Type	Ascending sagittal with A/P phase encoding direction
Voxel Size	1 mm isotropic
FOV	256 mm
Repetition Time (TR)	1540 ms
Echo Time (TE)	2.34 ms
Acquisition Time	216 seconds
Flip Angle	nine degrees
GRAPPA in-plane Acceleration Factor	2
Brain Coverage	Complete for cerebrum, cerebellum and brain stem

Table 2.1 Structural MRI acquisition parameters

Parameter	Value
Number of Slices	34
Slice Acquisition Type	Interleaved axial with A/P phase encoding direction
Voxel Size	3 mm, 3 mm, 4 mm
FOV	240 mm
Repetition Time (TR)	2000 ms
Echo Time (TE)	30 ms
Acquisition Time	308 seconds
Flip Angle	Ninety degrees
Multi band Acceleration Factor	2
Brain Coverage	Complete for cerebrum, cerebellum and brain stem

Table 2.2 Resting state fMRI acquisition parameters

nothing in particular.The parameters for acquiring resting-state data were as follows:

(c) **Task MRI Data**

Five sessions of T2* weighted echo planar fMRI data were acquired during stimulus presentation, lasting 5.1 minutes maximally per session. Each session consisted of a different paragraph, ordering randomized across subjects. The parameters for acquiring the fMRI data were as follows:

2. **Eye-Tracking Data Acquisition**

Eye movements of the participants were recorded using Eye-Link 1000 Plus long-range mount MRI-compatible eye-tracker (SR Research, 2016). The sampling rate of the eye-tracker was 1000 Hz and was mounted on the rear end of the

Parameter	Value
Number of Slices	30
Slice Acquisition Type	Interleaved axial with A/P phase encoding direction
Voxel Size	3 mm, 3 mm, 4 mm
FOV	240 mm
Repetition Time (TR)	**400 ms**
Echo Time (TE)	30 ms
Acquisition Time	Varied with the self-paced reading speed
Flip Angle	Thirty-five degrees
Multiband AF for Parallel Slice Acquisition	6
Brain Coverage	Missed top the parietal lobe and lower cerebellum

Table 2.3 Task fMRI acquisition parameters

scanner bore, capturing the eye movements from the reflective mirror above the MRI's head coil, monocular from the right eye. The participant's head was stabilized in the head coil, with the distance between the reflective mirror and the participant's eye being 120 cm. A 13-point calibration routine preceded the experiment, followed by the validating re-calibration before each reading session if the drifting error crossed one degree.

3. **Behavioral Data Acquisition**
   Participants were tested for general cognitive measures such as attention, working memory, and analogical reasoning. Additionally, they were asked to fill out a questionnaire on their reading habits (Reading Background Questionnaire) and their level of familiarity with the scientific subjects.

   (a) **Cognitive tests**

      i. Gray Silent Reading Test (GSRT) to test the level of reading comprehension competence. Thirteen narrative texts were read, and five assessment questions at the end of every text.

      ii. Raven's Progressive Matrices measure analogical reasoning in which participants choose the missing part from the options that complete the matrix to relations. The test was repeated sixty-five times in ten minutes and was based on different themes like continuous patterns and permutations of figures.

      iii. Letter Number Sequencing (LNS) tests the working memory by asking participants to recall the sequence of numbers in ascending order and letters in alphabetical order with an increasing number of sequences to remember.

iv. Attention Network Test (ANT) checks the attention span and the inhibitory control of executive functions. Participants were subjected to the Flanker test, in which they had to press the button corresponding to the central arrow flanked by either congruent or in congruent arrows. The reaction time was reflective of the inhibitory control.

v. Tower of Hanoi (TOH) measures key executive functions, the task is to correctly arrange the disks on a peg in the increasing order of size.

vi. Peabody Picture Vocabulary Test (PPVT-4) measures participant's vocabulary size. Participant has to match the word presented aurally with the picture presented on the screen from a set of options.

(b) **Reading Background Questionnaire**
Experimenters framed the questionnaire to test the reading habits on electronic media, time spent on reading and the preferred reading materials.

(c) **Familiarity Test**
Participants were asked to rate themselves on the Likert scale of 1-5 (1 being least familiar and 5 being the most) their level of contextual familiarity with the given domain of science. The subjects asked for were mathematics, astronomy, technology, environmental sciences and engineering. A point to note here is that the participants rated based on how well they knew the subject, not how well they understood the paragraph presented during the task fMRI for the same scientific subject.

2.2 Experiment design

2.2.1 Naturalistic Stimuli

It has been long debated whether the activation are because of the task or conditions during the experiment. Recently, with more studies studying the naturalistic paradigms, the results are coming out to be significantly different from the non-naturalistic settings. E.g., the activation in the multi-demand network during the next word prediction task was because of experimental settings; compared with the results from a naturalistic study, only the domain-specific network showed robust activation. The data used in this study follows a naturalistic paradigm to eliminate any effect because of experimental scenes, wherein the subject reads sentences (instead of single words in RSVP) in a self-paced manner. Combining fMRI with eye-tracking data and the high sampling rate makes post-hoc analysis poised with naturalistic scientific text comprehension.

2.2.2 Fixation-related naturalistic fMRI paradigm

Simultaneous eye-tracking and fMRI acquisition in language-related paradigms is used to study self-paced eye movements and explicate the precise onsets of words. In this study, native English speakers read five scientific paragraphs presented one sentence at a time in contrast to prevalent RSVP word-by-word presentations to set up a more naturalistic paradigm. On top of that, participants were allowed to pace the paragraphs with their individualistic reading speeds to avoid induction of cognitive load due to artificial lab settings.

2.2.3 Participants

Fifty-two adult native English speakers were recruited from Pennsylvania State Hershey Medical Center. All participants had normal or corrected to normal vision, were right-handed, and had no mental or neurological disorder history. Two participants did not complete the behavioral tests, hence, excluded from the analysis leaving the pool of 50 participants. Twenty-six among them were females with a mean age of 23.19 years (S.D. = 4.57) and the males had a mean age of 22.54 years (S.D. = 4.92).

Refer to figure 2.1 for the age demography of participant of population. Earlier, sixty-two subjects were recruited for the experiment, but ten were excluded based on handedness scores and in-scanner technical issues. Pennsylvania State University Institutional Review Board approved the ethical standards of the study, and the participants signed the written consent before they participated in the experiments.

2.2.4 Materials

Five scientific, expository texts were selected from a previous study conducted by the same group. Texts were modified to have the same linguistic characteristics with the 62.48 mean (SD = 1.92) character count per sentence, including the spaces and the 10.4 mean (SD = 0.62) number of words per sentence. Also, the number of sentences in each paragraph, word length and familiarity with the content words were kept nearly the same to avoid variability in the processing due to differences in lexical properties of the paragraphs. STEM texts chosen for the reading task were from subjects:

1. Text ID 1 - Astronomy (on Mars with 31 sentences and 310 words)
2. Text ID 2 - Environmental Science (on Supertanker with 31 sentences with 302 words)

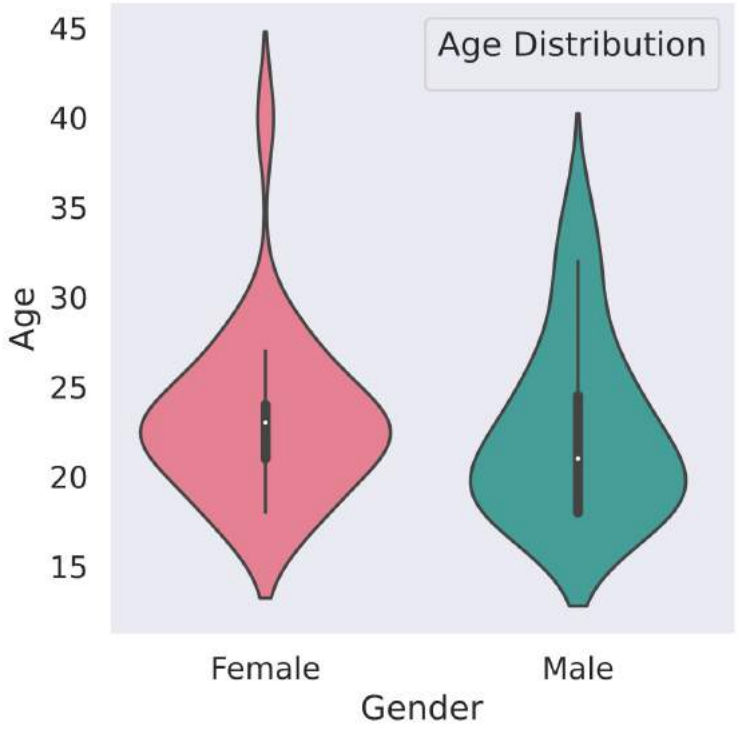

Fig. 2.1 Age distribution of the participant population, here the shape of the bar represents the distribution, the box and the whiskers represent the inter-quartile range and the adjacent values respectively

3. Text ID 3 - Mathematics (on Permutations and Combinations with 28 sentences, 306 words)

4. Text ID 4 - Technology (on GPS with 28 sentences and 307 words)

5. Text ID 5 - Engineering (on Electric Circuits with 30 sentences and 302 words)

Psycho-linguistic variables of the lexical properties are derived from the English Lexicon Project, the Kuperman-age-of-acquisition (AoA) database, the MRC Database and the Brysbaert concreteness database

2.2.5 Experimental Procedure

The experiment was completed in two sessions, one week apart. The first session comprised all the scanning procedures, and after one week, participants completed the latter half, consisting of behavioral tests. Refer to fig 2.2

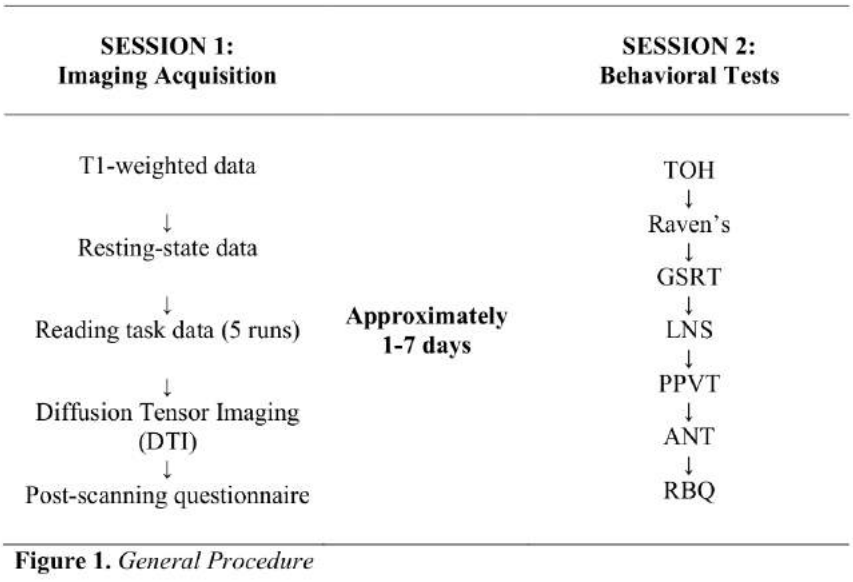

Fig. 2.2 Procedural overview of imaging and behavioral data acquisition

The chronology of the first half (Image Acquisition) was as follows:

1. Six minutes of structural scan

2. Five minutes long resting-state scan

3. Five reading tasks with simultaneous eye-tracking and fMRI (see the stimulus section for the timeline of the task data acquisition)
4. Diffusion tensor imaging (DTI)
5. Post-scanning questionnaire to assess the participants' experience and feelings during the scan.

The chronology of the second half (Behavioral Tests) recorded after a week of image acquisition is as follows:

1. Tower of Hanoi task
2. Raven's Progressive Matrices
3. Gray Silent Reading Task
4. Letter-Number Sequencing
5. Peabody Picture Vocabulary Task
6. Attention Network Task
7. Reading Background Questionnaire
8. **Familiarity ratings of the scientific subjects**

2.2.6 Stimulus

The stimulus was presented using E-prime 2.0 sentence by sentence onto the screen, and was projected on the reflective mirror mounted on the scanner at the participant's eye level. The task constituted an in-scanner practice session, followed by reading five self-paced scientific paragraphs and answering ten MCQs at the end of each paragraph. The order of the paragraph was shuffled for every participant. One could click the response button to shift to the following sentence once finished reading before the 8 seconds. After the eight-second time interval, the next sentence appeared automatically on the screen, and the eight seconds window was found sufficient to complete reading but not too long to cause boredom.

Below is the timeline for the simultaneous fMRI and eye-tracking reading task after the in-scanner practice session:

1. Eye-tracker calibration prevailing for varying time duration

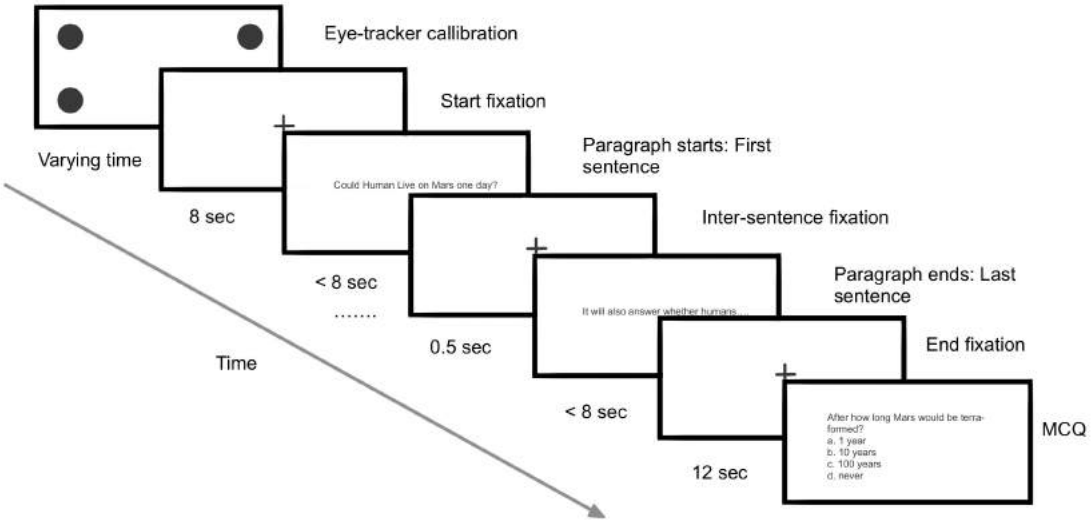

Fig. 2.3 Stimulus design: Procedural overview of one paragraph with eight and twelve seconds of fixation and variable sentence reading time, not more than 8 second

2. Start fixation lasting for sixteen seconds (dissimilarities found when discussed with authors, fixation duration calculated from onset files was found to be eight seconds)
3. First sentence presented for at most eight seconds
4. Inter-sentence fixation of half a second
5. Next sentence presentation again for not more than eight seconds
6. Inter-sentence fixation for half a second
7. Presentation of the last sentence ended by the subject at or before eight seconds
8. Sixteen seconds of end fixation
9. One minute for solving ten MCQs
10. After completing the multiple-choice questions, the eye-tracker calibration for the next paragraph began
11. Steps, as mentioned above, repeated for four more paragraphs

2.3 fMRI Preprocessing and Analysis

2.3.1 Preprocessing

Preprocessing was done using SPM12 v6909 (Friston et al., 2007). Steps included susceptibility artifact correction, realignment, co-registration, segmentation, normalization and smoothing (Glasser et al., 2013b). The slice time correction step was excluded as the multi band, and low TR acquisition enables the acquisition of a large number of slices in a very short period for whole-brain coverage. Hence, it reduces the need for slice time correction as the first and last slices in the volume are acquired much closer than the typical fMRI acquisitions (TR 2.5 s). The differences in the raw and the preprocessed MRI images can be seen in figure 2.5. The steps used were as follows:

1. Correction of in homogeneity artifacts in functional images using Hyper-elastic Susceptibility Artifact Correction (HySCo) toolbox utilizing a pair of spin-echo sequence images acquired opposite phase encoding gradients. While EPI is the commonly used ultra fast acquisition technique, it has a significant drawback of being highly sensitive against small magnetic field perturbations due to the differential magnetic susceptibility of different tissue types. One can correct these distortions by reversing using the pair of spin-echo with opposite phase directions as it changes the direction of the magnetic field in homogeneity effects on images (Glasser et al., 2013a).

2. Realignment (estimate and re-slice): All functional volumes were corrected for head motion artifacts with a quality of 0.9 and registered to the mean image

3. Co-registration (estimate and re-slice): The structural images were co-registered with the functional volumes, with the structural image being the source image and the functional image as the reference image

4. Segmentation: The co-registered structural images are then bias-corrected and segmented according to the tissue type with the forwarding deformation field

5. Normalization (write): Structural and functional images were warped and normalized with MNI template volumes with 2 x 2 x 2 resolution

6. Smoothing: All warped volumes were selected to smooth with FWHM of [8 8 8].

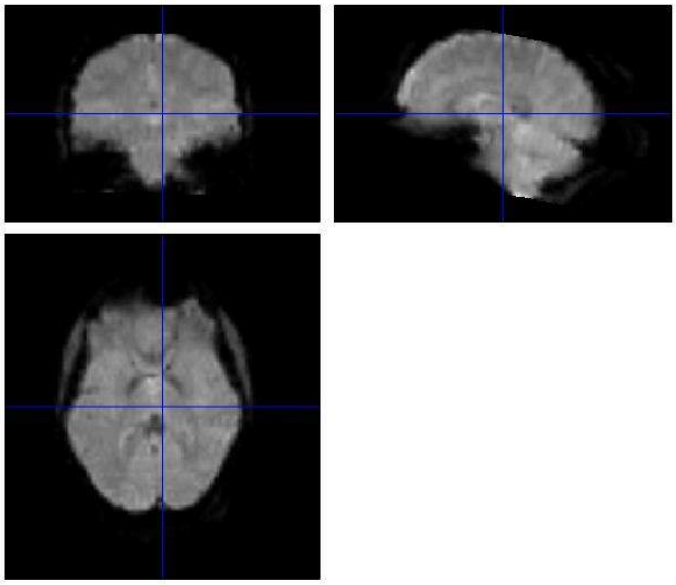

Fig. 2.4 Raw fMRI image: MRI slices (sagittal, axial and coronal) without any preprocessing displayed on SPM12 image window

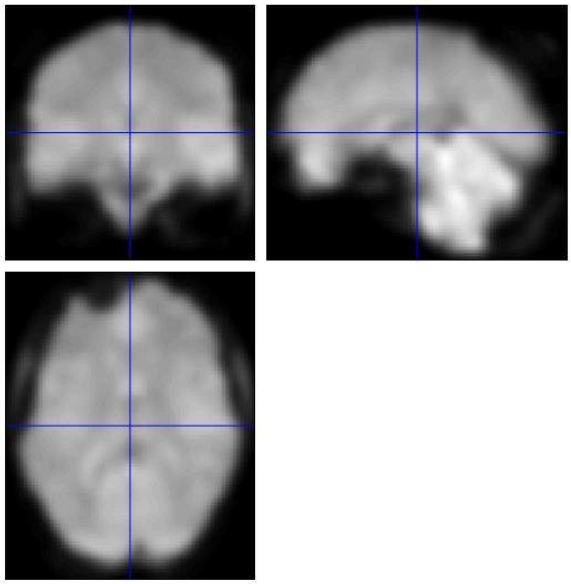

Fig. 2.5 Preprocessed fMRI image: MRI slices (sagittal, axial and coronal) after the susceptibility correction and the SPM preprocessing steps (realignment, co registration, normalization and smoothing)

2.3.2 Functional ROI

The study is confined to seeing the changes only in the regions previously reported to involve language tasks. The GLM and functional connectivity analysis parcels are functional ROIs, first written by Evelina Fedorenko (Fedorenko et al., 2010) Initially, the parcels were defined by Evelina Fedorenko's group using the group constrained subject-specific (GSS) method, which was as follows: They created subject-specific maps for thresholded activation in sentence>non-words fMRI localization tasks; they then overlapped these maps for all subjects. Then this overlap was divided into "group-level partitions" following the topographical information in the map, using the watershed algorithm, an image segmentation algorithm. This algorithm works by finding the local maxima, the "watershed ridge", and the surrounding "drainage basin," the neighboring voxels to the local maxima; working by incorporating one voxel at a time with decreasing intensity of the voxel as it goes down towards the "catchment area." Here, the voxel's intensity is determined by the probability of it being activated across all the subjects. In the partitions in which an activity probability of 0.8 was selected, 16 group level partitions met the criteria. After studying across several years, these 16 parcels were modulated, merged, and sub-divided into 12 parcels in later studies.

Our study focuses on these twelve parcels, and the activation reported is confined to the partitions. We did not use the last step of functional localization, wherein subject-specific ROIs are demarcated within this group level partition; instead, we considered this group's functional ROIs to be simple atlas-like, usually used during fMRI analyses. These twelve functional ROIs as shown in figure 2.6 were:

1. The orbital part of the inferior frontal gyrus, left and right
2. Inferior frontal gyrus, left and right
3. Middle frontal gyrus, left and right
4. The anterior temporal lobe, left and right
5. The posterior temporal lobe, left and right
6. Angular gyrus, left and right

Brain Region	Abbreviation
Inferior Frontal Gyrus Orbital	IFGorb
Inferior Frontal Gyrus	IFG
Middle Frontal Gyrus	MFG
Anterior Temporal	AntTemp
Posterior Temporal	PostTemp
Angular gyrus	AngG

Table 2.4 Regions of interest and the corresponding abbreviations

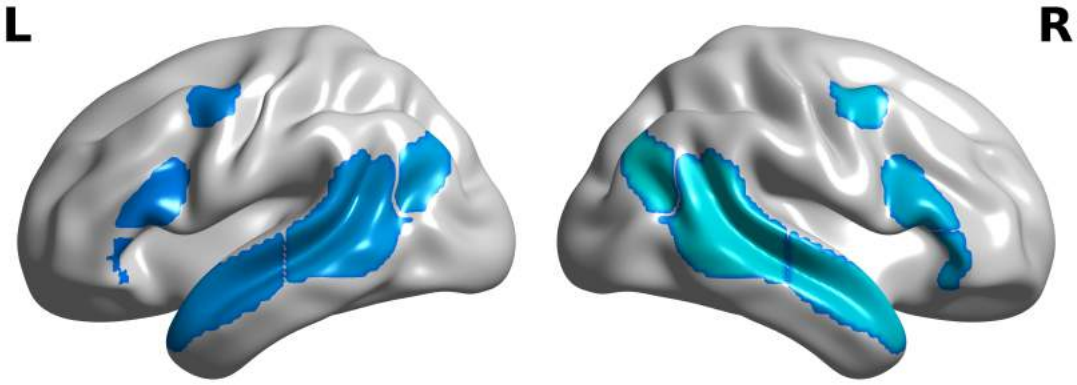

Fig. 2.6 Twelve Language Parcels: ROIs defined by group-constrained subject-specific method for sentence > non-words contrast, in the left and right inferior frontal and temporoparietal regions

2.3.3 Analyses

Each paragraph read by participants had a paragraph ID (unique for each scientific subject) and was presented in random order to every participant. Every paragraph for each participant also had a corresponding familiarity score. These paragraphs were divided based on the familiarity score resulting in five groups from the same sample population; for every familiarity score. We then, using the same five groups, divided our analysis into two parts:

1. Group average t-map and comparing the between groups' activation patterns
2. Group average weighted functional connectivity and compared the changes in functional connectivity in the language-specific areas with changing familiarity.

In the first part of the analysis, we computed the quantitative measures of the activity, like regions with supra-threshold activity, the t-value and beta values quantifying the strength of the activation, and the number of voxels involved in a particular

ROI amongst groups. In the second part of the functional connectivity analysis, we measured the qualitative changes in the network and the inter and intra-hemispheric communication between the regions. The strength measures of the connection between two regions were reported using the correlation coefficients.

GLM Analysis

Background:
General linear model is one of the methods to estimate the voxel-wise activation in different conditions. The signal, BOLD time-series, is modeled in terms of explanatory variables, known as regressors. It tries to explain a series of measurements using the regressors (series of measurements associated with individuals in a group) that represent patterns that we expect to be found in the measured signal. The linearity is because it scales the regressors and adds them together, linearly. And not because it can only model straight lines, many GLMs measure a more complex relationship between subject and/or time. The scaling value is known as parameter estimate or the beta value and determines the difference (or the residual error) between the data and the scaled regressor (the fitted model).

The GLM can be represented by the equation

$$Y = X\beta + \epsilon \tag{2.1}$$

where the Y represents the BOLD time series of a voxel, X is the matrix of regressors (design matrix), β represents the matrix of the scaling parameter and ϵ is the residual error or unexplained variance (noise).

Once the image with value in every voxel representing the voxel-wise parameter estimate, known as beta maps, is created, a t-test is run to commute the difference between conditions. This thresholded voxel-wise t-test results images are known as t-maps.

The activation level can be quantised using parameter estimates, the t-value or the percentage signal change. Statistical meaning of different currencies for the level of activation:

1. **Parameter estimates:** The beta or the slope value best fits the convolved HRF model to the voxel time series, minimizing the squared error.

2. **T-value:** At the voxel level, the one-sample t-test is done on the parameter estimates to examine whether the activation levels differ between two conditions at a specific confidence interval.

3. **Percent Signal Change:** The standard Marsbar method (used in this analysis) is to reconstruct the time course for the fitted event for a given duration and use the maximum of this time course as the numerator multiplied by a hundred. **We calculated percent signal change using the MarsBaR's auto-correlation method instead of default restricted maximum likelihood method due to some unidentified errors.**

Multiple Comparison Problem

Type I error rate is the probability of rejecting a null hypothesis given it is true, false positive. The Type II error rate is denoted by the probability of accepting the null hypothesis when it should be rejected, false negative.
In fMRI, many voxels undergo hypothesis testing simultaneously, and the chances of Type I error are very high; this is called a multiple comparison problem. Various methods have been developed to address this issue; these are:

1. **Bonferroni's correction:** Divides the nominal significance level by the number of tests performed. It disadvantageously removes both false and true positives.

2. **Family-wise error (FWE) correction:** It is based on Random Field theory and assumes that the error fields can be a lattice approximation to an underlying random field.

3. **False Discovery Rate (FDR) correction:** This method is more sensitive and less likely to produce Type II error than the FWE correction method. It only focuses on the expected proportion of false positives among surviving voxels FWE, which considers all false positives. Hence, we corrected all our results using FDR correction at $p < 0.05$ (Han and Glenn, 2018).

GLM Procedure

After preprocessing, we did subject-specific, first-level general linear modeling to calculate the voxels showing a significant activation for sentence reading than fixation.
The two conditions, fixation, which was 6 and 10 seconds long, before and after the paragraph and the sentence reading, which had varying duration (because of self-paced reading), were compared. The second condition's inter-sentence interval of 0.5 s was neglected and was not regressed. The design matrix in figure 2.8 consisted of two regressors of interest, fixation and sentence reading and six motion parameters as a

regressor of non-interest. We applied a high band-pass filter with a cut off period of 128 s; we used the SPM12 FAST option for temporal auto-correlation (Todd et al., 2016).
The FAST option, newly introduced, allows for an improved correction for non-sphericity due to temporal auto-correlation. It is particularly relevant for short TR studies where traditional auto-correlation and white noise models fail to account for physiological noise optimally. Lastly, a one-sample t-test was done to contrast conditions, sentence and fixation. A second-level analysis of a random effect one-sample t-test was done on the group with the same familiarity score to compute the activation for sentence>fixation. We applied peak level false discovery rate (FDR) correction at $p < 0.05$ and a cluster threshold of zero to generate group, brain-wide t-maps. Since familiarity groups number four and five had 38 and 21 subjects, respectively, we merged these two into one single group with 59 sessions to avoid sample number bias. Please refer to figure 2.7 for the distribution of subjects across the groups. Since the number of sessions in each group is remarkably different, we randomly sampled forty-eight sessions from each group, equalizing the sample size.

Functional Connectivity Analysis

There are many different ways to measure functional connectivity for fMRI studies. We were interested in studying the connectivity changes within the language regions with the changes in the contextual familiarity to find the bio-marker for the knowledge base. We chose the weighted ROI to ROI connectivity measure, limited language ROI, which is pairwise connectivity between only the pre-defined ROIs, unlike asymmetric seed-based connectivity.

Weighted RRC measures the task or condition-specific functional connectivity among pre-defined ROIs. They are computed using the Weighted Least Squares (WLS) linear model with user-defined temporal weights identifying each condition. A matrix of the bi-variate regression coefficient for each condition is then transformed to Fisher correlation values for each ROI and is entered into the t-test. The matrix is color-coded according to these T-test results.

In the figure 2.9 the 'R' is the ROI time series, 'w' is the temporal weighting function, 'h' is the task boxcar time series, 'f' is the hemodynamic response function, 'B' matrix of bi-variate regression coefficients for each condition estimated using a

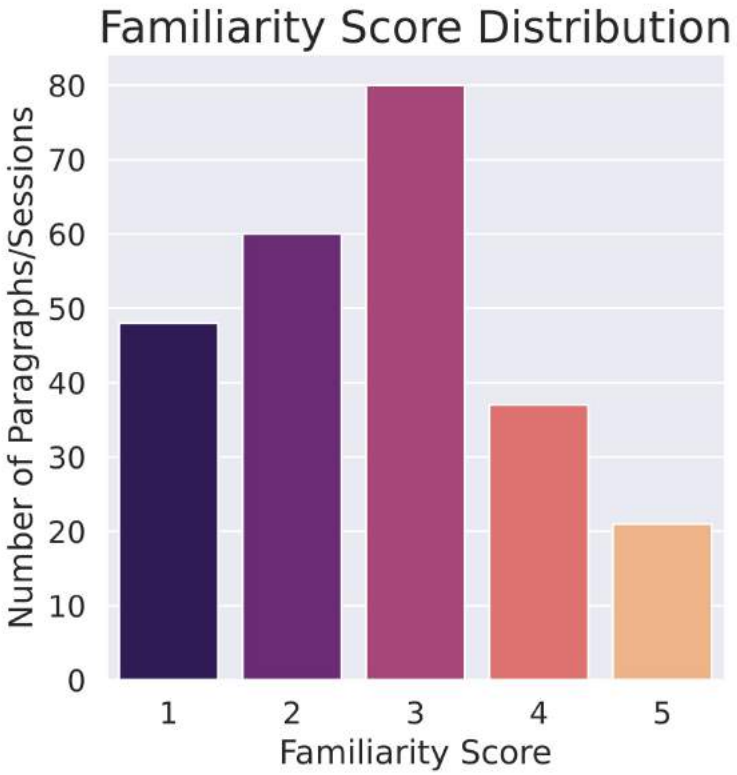

Fig. 2.7 Distribution of subjects in each familiarity group

Weighted Least Squares (WLS) solutions to the linear model, and 'Z' is the wRRC matrix of Fisher-transformed bi-variate correlation coefficients for each condition.

Denoising the ROI-wise time series: In addition to minimal preprocessing in the SPM12, we performed denoising on ROI time-series. It includes linear regression of potential confounds in the BOLD signal and temporal bandpassing. The ordinary least square method (OLS) identifies potential confounds from cerebral white matter and cerebrospinal areas and regresses them. During temporal bandpass filtering, canonically frequencies below 0.008 Hz and above 0.09 Hz are removed to avoid the influence of low-frequency noise. **We wanted to exploit the fast acquisition of the fMRI as described in the introduction. Therefore, we kept the denoising window below 0.01 Hz and above 0.5 Hz.**

FC Analysis Procedure

We used MATLAB based CONN toolbox (Whitfield-Gabrieli and Nieto-Castanon, 2012) to measure weighted ROI to ROI functional connectivity, dividing the pool of

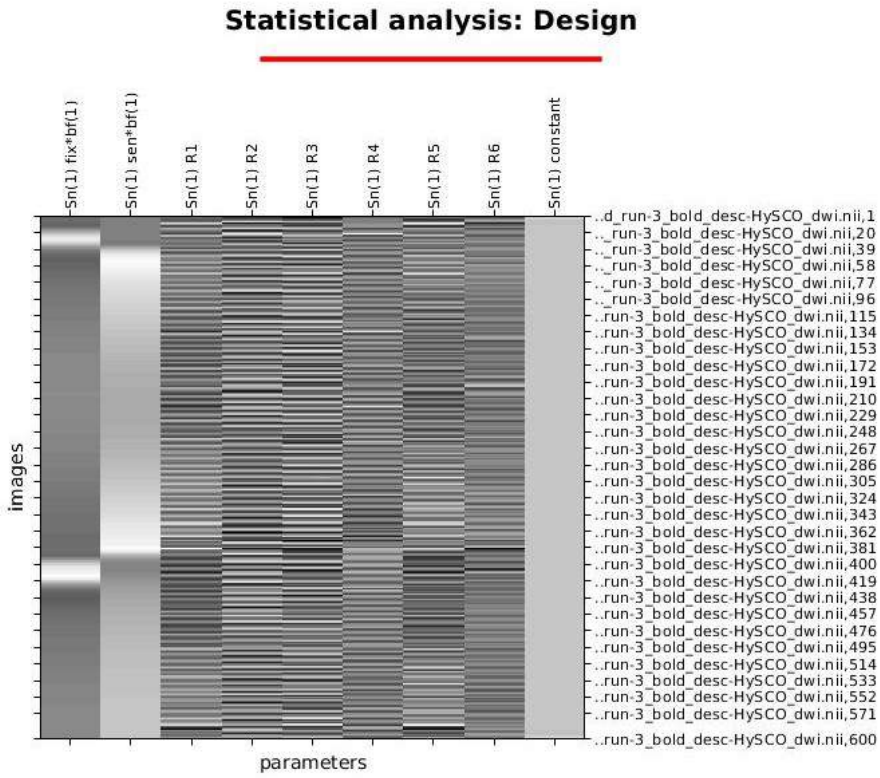

Fig. 2.8 Design Matrix for first level analysis with fixations in column one, sentence reading in column two and motion correction regressors in next six column and baseline or average in the last

participants into four groups of equal sample numbers with similar familiarity scores. We merged participants with familiarity scores of four and five.

First Level Analysis

The subject-specific design matrices were imported from SPM.mat files after the ROI-wise denoising of the functional file. At the first level, weighted (for sentence reading condition) functional connectivity was calculated ROI-wise for every subject. **Second Level Analysis**

CONN produces while computing a standard second-level GLM, a single group-level T-matrix, characterizing the values of interest (sentence reading in our case). We then implemented standard functional network connectivity (FNC) multivariate parametric statistics (Jafri et al., 2008) at the cluster level. Cluster-level inferences divided the ROI based on the functional similarity and anatomical proximity matrices using the hierarchical clustering procedure (complete linkage clustering).

$$R_j(t) = \beta_n(i,j)R_i(t) + \epsilon_{i,j}(t)$$

$$\beta_n(i,j) \mid \min_{\beta_n(i,j)} \int w_n^2(t)\epsilon_{i,j}^2(t)dt$$

$$w_n(t) = [h_n(t) * f(t)]^+$$

$$Z_n(i,j) = tanh^{-1}\left(\beta_n(i,j)\, c^{1/2}\right)$$

$$c = \frac{\int R_i^2(t)dt}{\int R_j^2(t)dt}$$

Fig. 2.9 Formulae for calculating weighted functional connectivity

After clustering, the algorithm runs a multivariate parametric General Linear Model (GLM) for the entire set of connections within and between the clusters. Additionally, we manually defined two clusters comprising left and right language regions from the ROI parcels, which we used in our complete analysis and re-ran the cluster-based inferencing to check the differences between left and the right hemispheric connections.

The FNC results in an F-statistic for each pair of connections, and an associated FDR corrected p-values, thresholded at $p < 0.05$.

These ROI-to-ROI parametric maps were scrutinized in the form of thresholded connectivity matrix, connectivity rings, and the connections on the 3D brain; for more details, see the methods section .

Significance FC tests:

- **ROI Pair-wise Analysis:**
  We also performed Welch's t-test between every group for every ROI pair. We compared the subject-specific Z-scored connectivity matrices across groups at a significance of 0.5. Furthermore, in search of the ROI-to-ROI connectivity changes between the group with familiarity scores one and four, we computed a one-tailed Welch's t-test for the ROI pair having higher connectivity in group one than four and separately to track higher connectivity measures in group four than one. We have teased apart the results in section .

Chapter 3

Results

3.1 Behavioural Analysis

Mean paragraph reading time was calculated for every group, including the 0.5 s inter-sentence intervals, refer to figure 3.1. We hypothesised that the reading time for texts with high familiarity to be lower. But, when performed pair-wise two-sample, two-tailed t-test the results show no significant difference between any two group.
Critical insights: Inter-quartile range is smaller for the group with a familiarity score of two among all the groups.

3.2 GLM Analysis

The following 3.2 are the second-level t-maps rendered on the inflated 3D brain for different familiarity groups with an equal number of samples (48 subjects in each group). The colour of every supra-threshold voxel depicts the t-values for the sentence > fixation contrast ,and the colour bar was adjusted to even up the scale for all four groups. The whole-brain (without masking) t-maps were FDR corrected ($p<0.05$) with the cluster threshold of zero. Figure 3.2 shows the left lateral view, and figure 3.3 shows the occipital regions of the brain.
Critical insights: Group with a familiarity score of one has more activation in the visual areas and the left IFG and MFG than a group with a score of four. Familiarity two (a group with a self-rated familiarity score of two) has significantly higher activation in the language-specific areas than any group; also, the left angular gyrus can be seen recruiting multiple voxels. No supra-threshold voxels were found in the right hemispheric

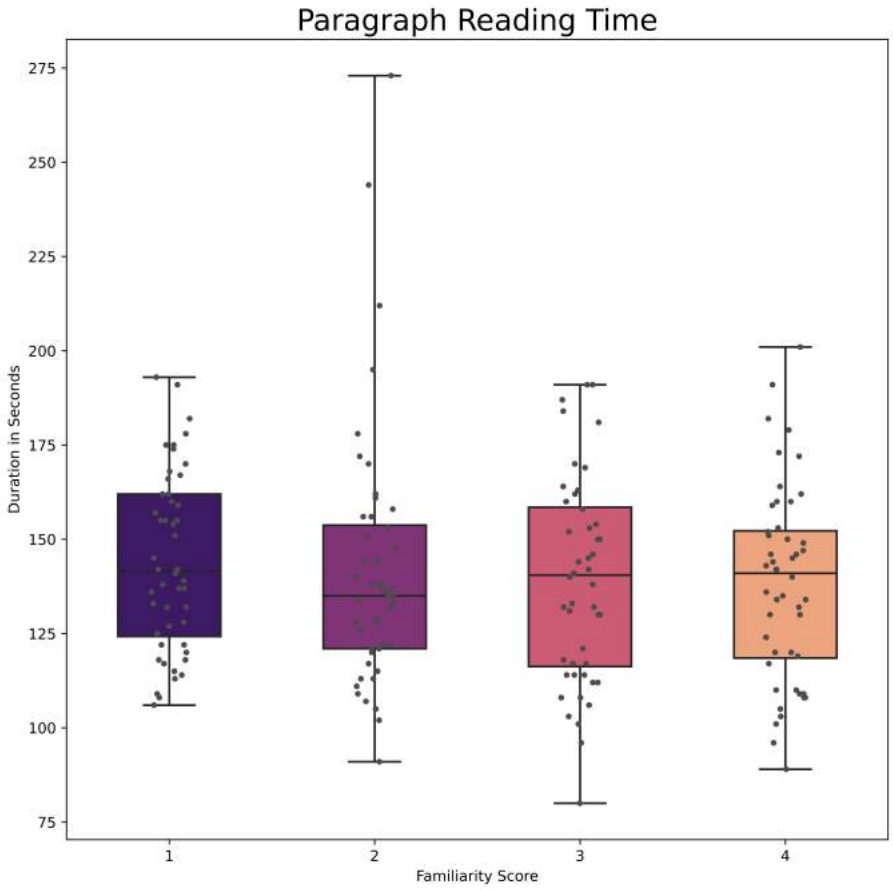

Fig. 3.1 Paragraph reading-time distribution for between groups where the central line depicts the median, box depicts the inter-quartile range and the whiskers depict the maximum and minimum value in the distribution, the x-axis represents the familiarity-group and the y-axis represents the time in seconds

homologous areas, reflecting the prominent left lateralization of the language processing (Frost et al., 1999).

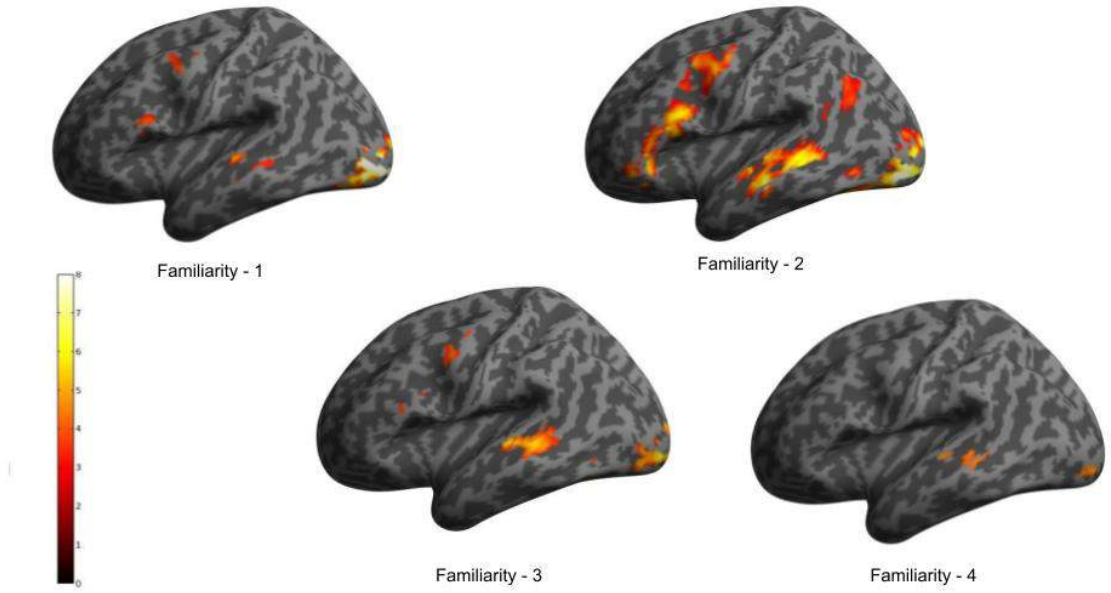

Fig. 3.2 Sagittal-lateral view of group-averaged t-maps rendered on inflated brain for each familiarity group, here the colorbar represents the T-value with the maximum value of 8.0 and the map on the surface represents the supra-threshold voxel with significance threshold of 0.05.

3.2.1 Percent Signal Change:

We chose the ROI level BOLD percent signal change during the task from the average activity (during the entire experiment) as the measure to report the changes in the BOLD signal. Refer to the figure 3.4, which shows the ROI wise mean (across participants) percent change in the left and right hemispheres, with the error bars depicting the standard error of the mean. We confined the analyses to the language-specific regions and traced the changes in them across increasing familiarity.

Critical insights: Left hemisphere has a positive (about 0.05% at most) percentage change for sentences > fixation, and the right homologes show negative but of the same magnitude (about -0.05% at most), again reflecting the involvement of left language-specific areas. The right negative BOLD response has been argued to be because of active inhibitions from the left domain-specific regions. See the discussions for more details on negative BOLD responses. Left areas, including the orbital part

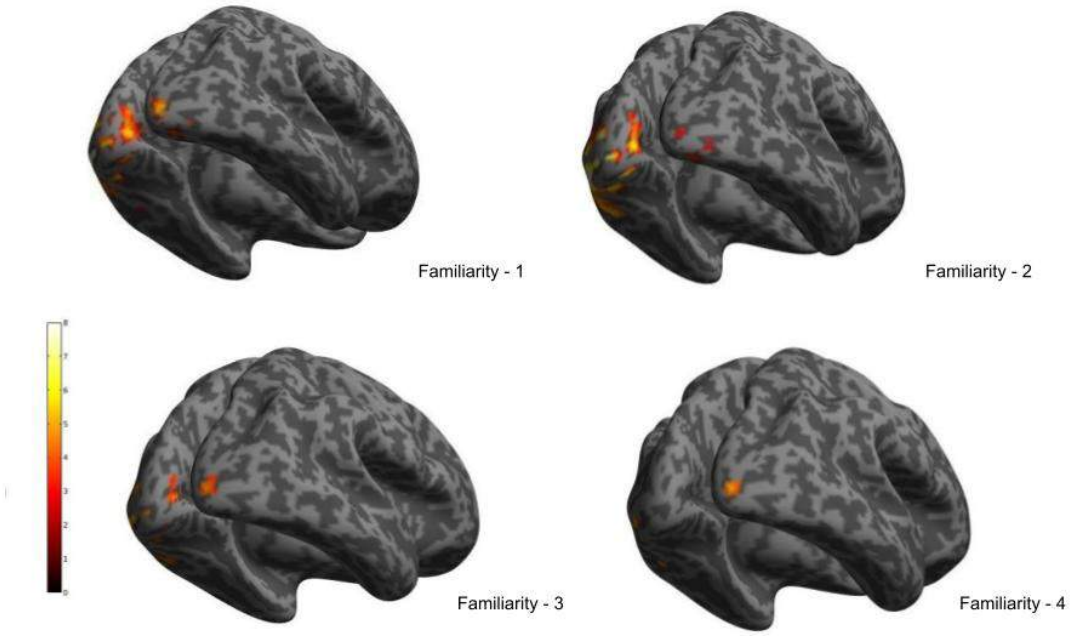

Fig. 3.3 Posterior view of second level t-maps rendered on inflated brain for each familiarity group, here the colorbar represents the T-value with the maximum value of 8.0 and the map on the surface represents the supra-threshold voxel with significance threshold of 0.05.

of the inferior frontal gyrus, the inferior frontal gyrus, the middle frontal gyrus, and the anterior and posterior temporal lobe, show a decrease in the magnitude with the increasing familiarity. The left angular gyrus displays the negative percent signal "behaving" much like the right regions' "family", and only the group with a familiarity score of two had the supra-threshold voxels in the region, which is reflected in the graph by the slight positive percent signal as compared to other groups. The malicious behaviour of the left angular gyrus has been discussed in more detail in discussions. Compared with the activation pattern in the t-maps, the bar plot unravels the baseline activity of different regions. For example, the left MFG shows up in all the groups except the last one. The percent change is positive - with varying magnitude - in all the groups, concluding that the baseline must exist somewhere near the percent activity of group four.

3.2.2 Number of Voxels in Language Regions

We calculated the number of voxels by masking the second level SPM.mat files by language ROIs for the four groups. In figure 3.6, the radius of the arcs characterises

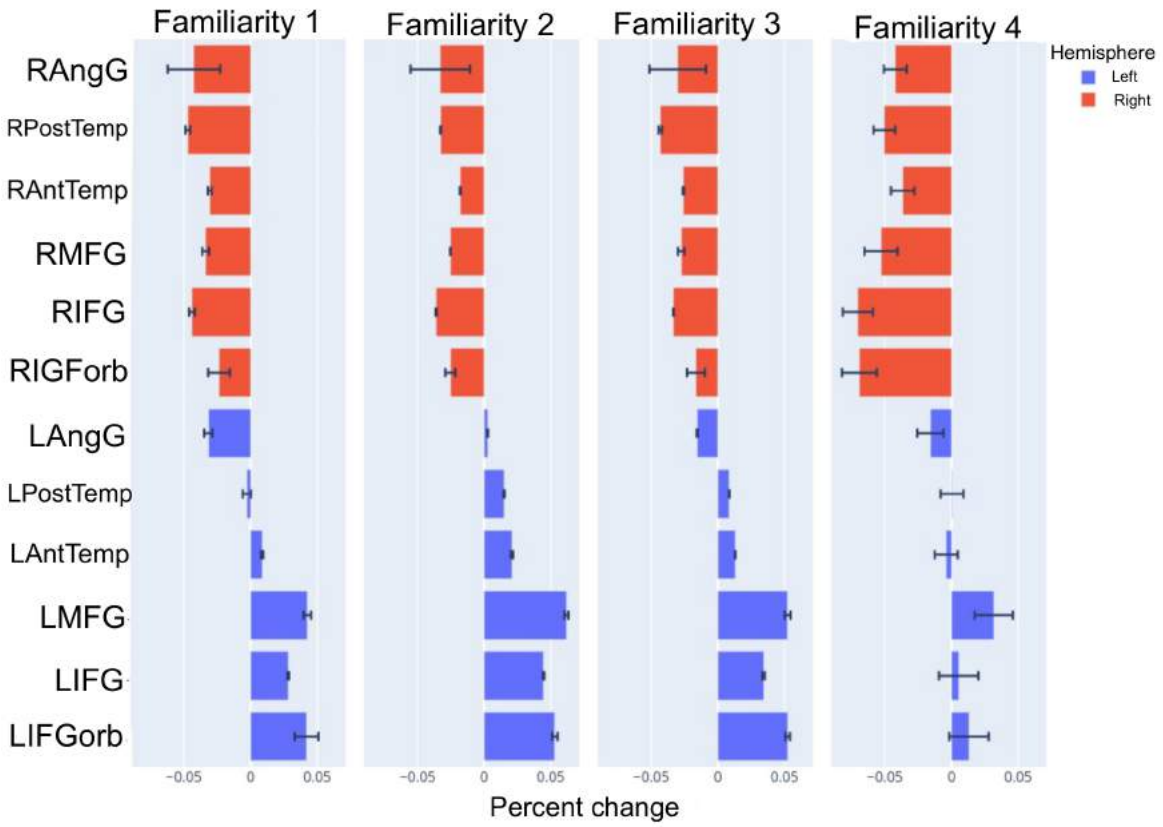

Fig. 3.4 Average percent signal change in language ROIs compared across groups with error bar representing the standard error of mean and the x-axis represents the percent signal change with range from -0.05 to 0.05, the categorical y-axis represents the ROI in the left and right hemisphere

the number of voxels, and the disc colour denotes the familiarity group.
Critical Insights: The second group activated the most number of voxels in mostly all the left domain-specific areas. The posterior temporal lobe can be witnessed to recruit the most significant number of voxels in all the groups.

3.2.3 T-values in Language Regions

The figure 3.5 below quantifies the strength of the activation, previously were visually depicted on t-maps. **Critical Insights:** The posterior region including the left posterior and anterior temporal lobes and the MFG have almost same T-values across groups, also, the left inferior frontal gyrus, which is a core language processing region, doesn't get activated at all in the fourth group.

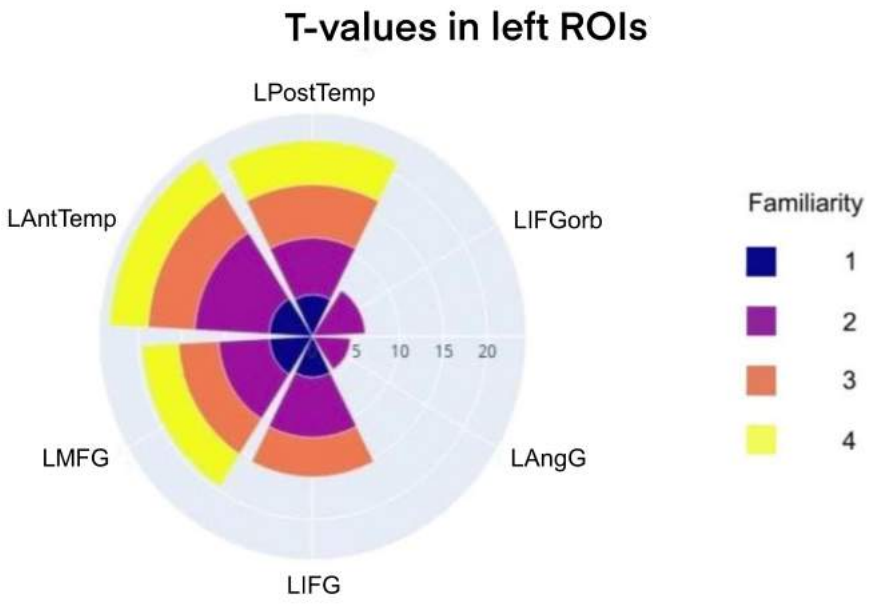

Fig. 3.5 T-values and corresponding language areas (left hemispheric) in familiarity groups where the annular width size represents the t-value and the familiarity group is represented by the colors, the scale is drawn on the radius (right hand side). These values were obtained from thresholded t-maps and ROI were defined using the ROI described in in the methods section.

3.2.4 Non-Language Areas

As shown in figure 3.7, some groups showed activity in areas other than the language network. Comparison for the number of voxels in these regions can be estimated from figure 3.8.

Critical Insights: Mainly supplementary motor area, which is known to be activated during silent reading, was well reported. The fusiform gyrus, which includes the visual word form area - the brain's letterbox - responsible for registering words early during the comprehension, was also activated in groups one and three. The other areas activated were the hippocampus and the left precuneus in group two and the left inferior occipital gyrus in group four.

The list of areas outside the language parcels were:

1. Left precentral gyrus (PreCGL)
2. Left fusiform gyrus (FFGL)
3. Hippocampus (Hippo)

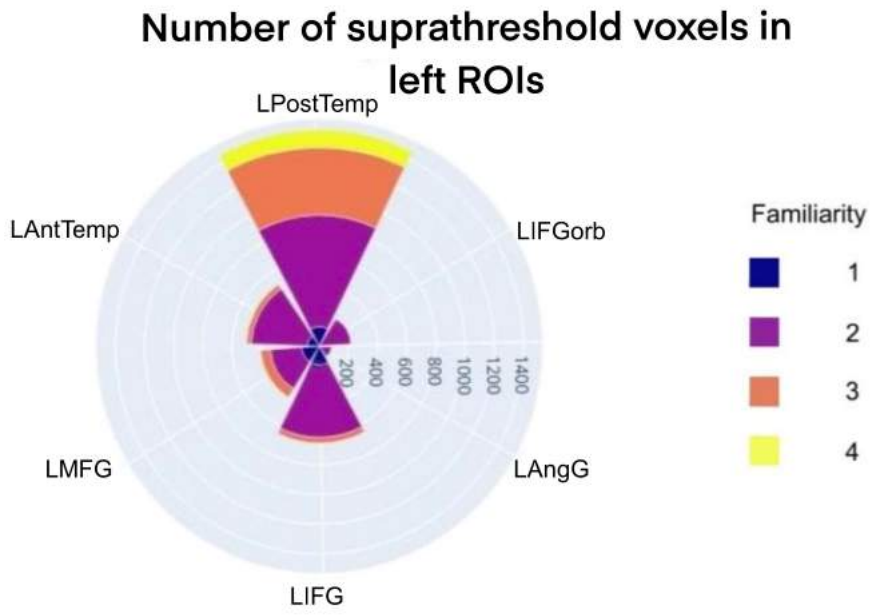

Fig. 3.6 Number of voxels and corresponding language areas (left hemispheric) in familiarity groups where the annular width size represents the number of voxels and the familiarity group is represented by the colors, the scale is drawn on the radius (right hand side). These values were obtained from thresholded t-maps and ROI were defined using the ROI described in in the methods section.

4. Left precuneus (PreCuL)

5. Left inferior occipital gyrus (IOGL)

3.3 Functional Connectivity Analyses

Connectivity Matrices

We characterized left and right language parcels as two clusters. Below is the figure 3.10 for the FDR corrected ($p<0.05$) colour coded correlation value between the ROIs in the form of a matrix. The range for the colour bars was from -25 to 25. We found the differences in the inter-and intra-hemispheric correlations while visually inspecting the matrices.

Critical Insights: Left intra-hemispheric connections were most robust in group two and least in group one. The inter-hemispheric connections between the left and right anterior as well as posterior temporal lobe remain consistent across groups. The right intra-hemispheric connections are least in group one and most in group four.

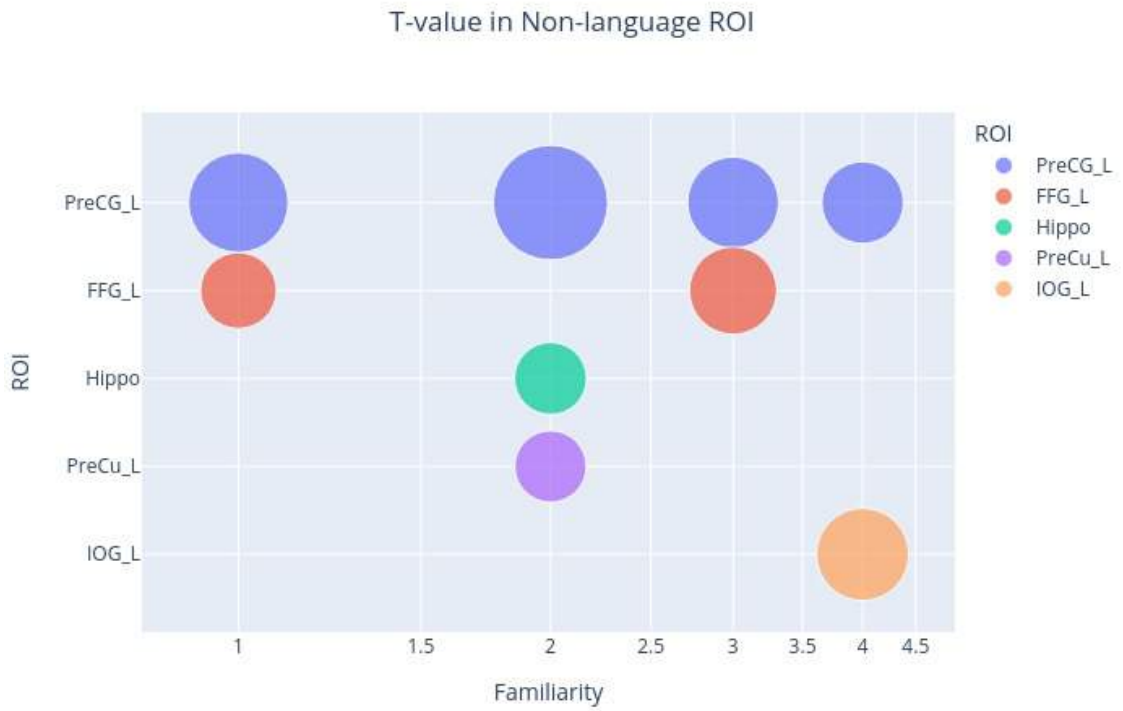

Fig. 3.7 T-values and corresponding non-language areas in familiarity groups, here the t-maps refer to the group-averaged t-maps and the areas were defined using neuromorphometrics atlas, pre-defined in SPM12. The radius of each bubble represents the t-values and the color represents the ROI, the x-axis and y-axis are familiarity score and the ROI, respectively.

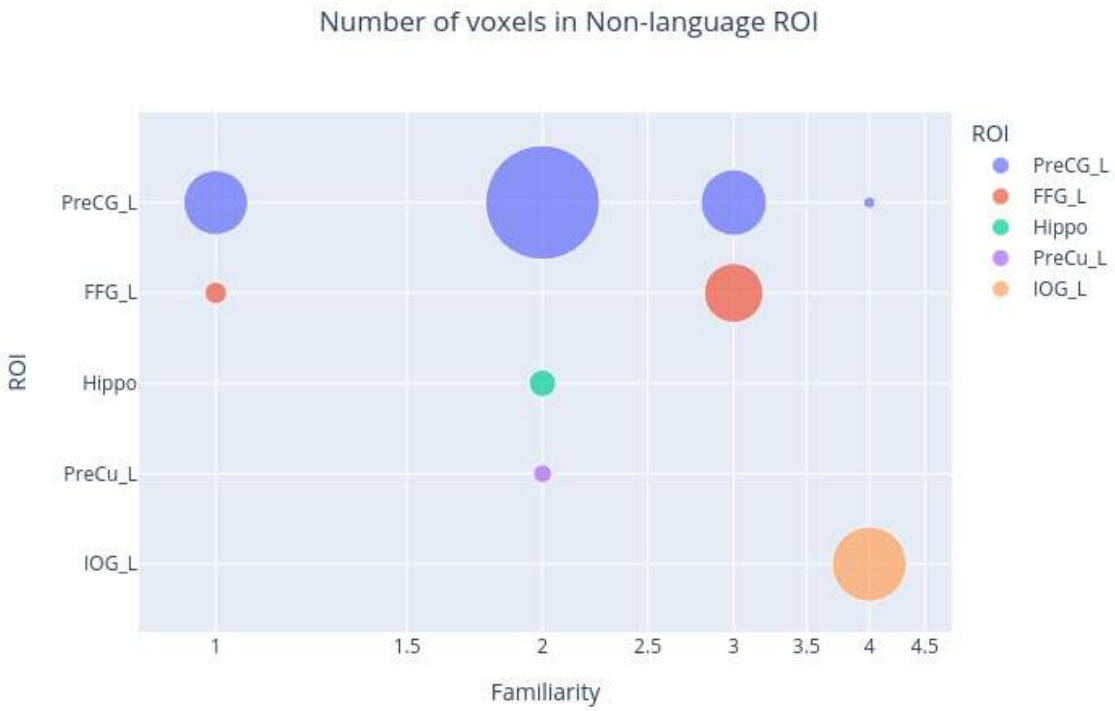

Fig. 3.8 Number of voxels and corresponding non-language areas in familiarity groups, here the t-maps refer to the group-averaged t-maps and the areas were defined using neuromorphometrics atlas, pre-defined in SPM12. The radius of each bubble represents the t-values and the color represents the ROI, the x-axis and y-axis are familiarity score and the ROI, respectively.

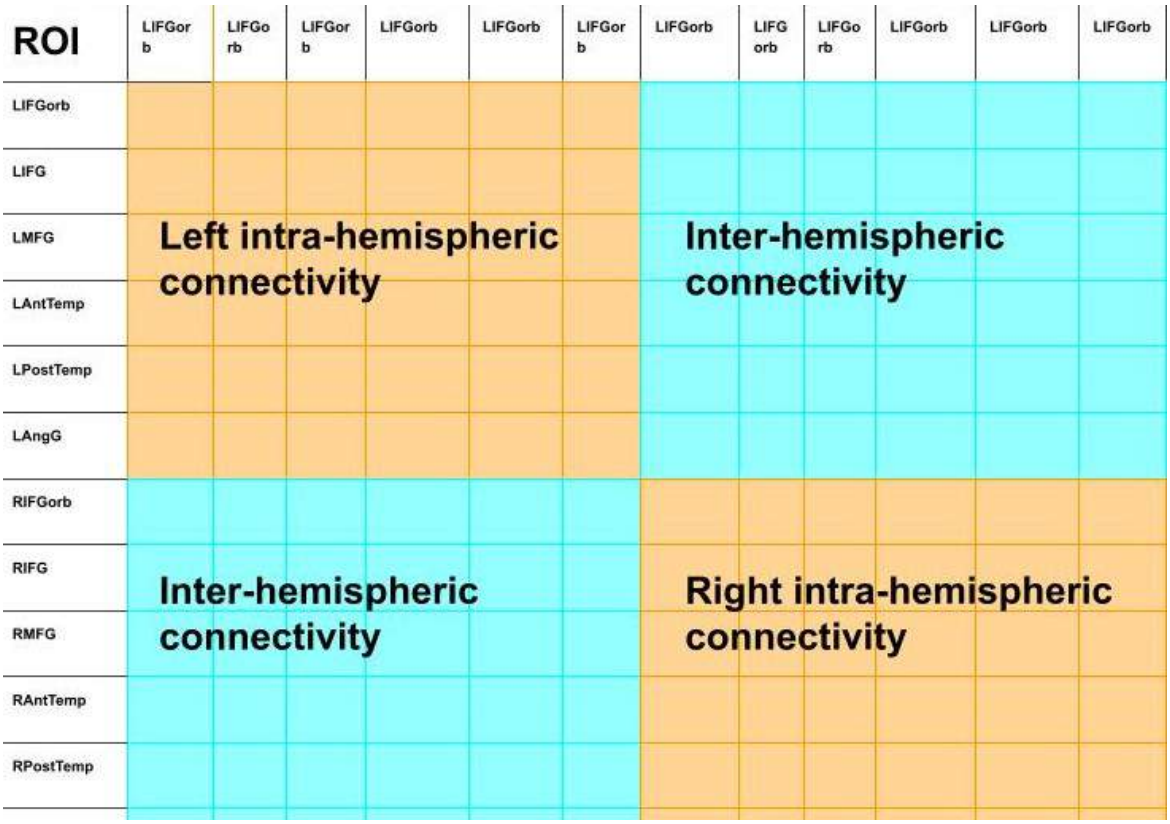

Fig. 3.9 ROI to ROI matrix to be used for the reference for inferring the intra- and inter-hemispheric connections with all the functional ROI in the language network used in functional connectivity analysis.

3.3.1 Connectivity Rings

The following are the CONN generated connectivity rings for all the significant connections figure , only the left hemisphere, figure , only the right hemisphere, figure and only the inter-hemispheric connections, figure .

Critical Insights: The inter-hemispheric connectivity ring, figure 3.15 shows that the posterior regions are more connected cross-hemisphere than the anterior regions. These posterior connections are more substantial in group one than in any group. Familiarity four has the least inter-hemispheric connections. The Left and right anterior temporal lobes are most strongly connected than any other pair in all the groups. There is a high anti-correlation in familiarity two between the left angular gyrus and the right orbital inferior frontal gyrus. From the figure 3.17 for only the intra- right-hemispheric connections, it is prominent that there is a high correlation between the right orbital inferior frontal gyrus and the right anterior temporal lobe persists except for the familiarity one. Also, the local connections are more in group

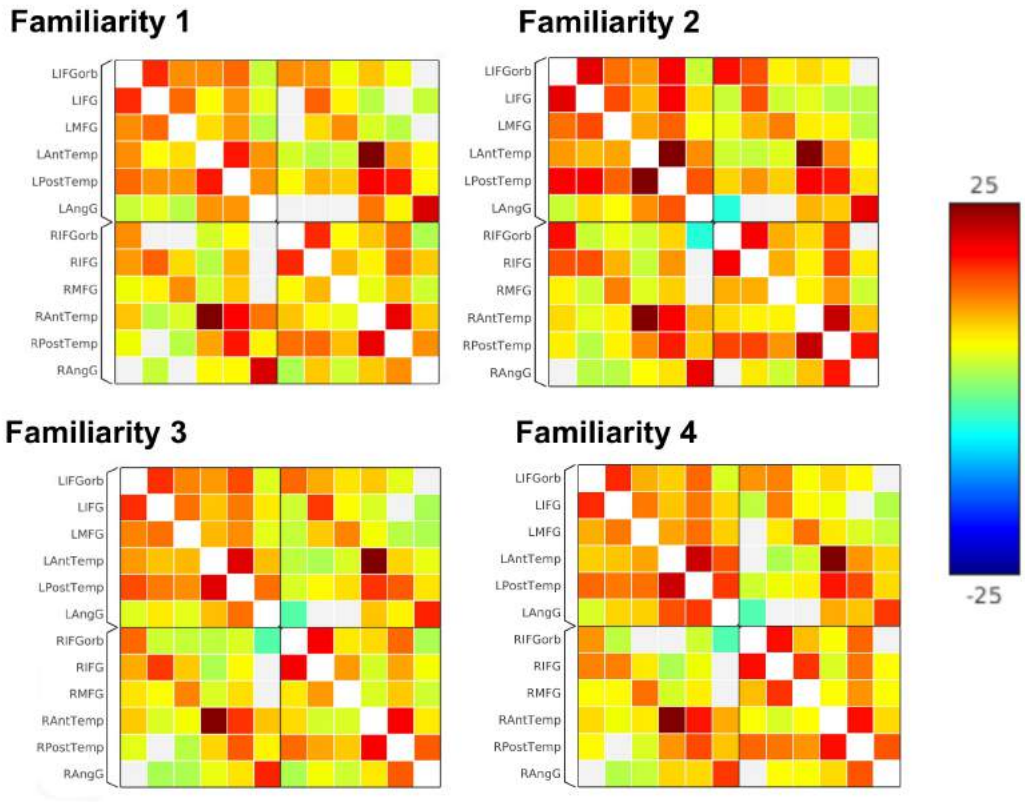

Fig. 3.10 Suprathreshold functional connectivity matrices with left and right hemispheres as clusters - group level, the significance threshold is at 0.05 and are color coded according to the z-scored correlation values with the range is from -25 to 25, the ROIs are the same twelve functional regions defined in the methods section.

four than in group one. The figure 3.16 displaying only the left hemispheric connections reveals that the strong local connections are present from group two to group four - without any significant changes. In contrast, they are very minimal in group one.

3.3.2 Connections on the 3D brain

The figure 3.19 shows the connections rendered on the model using CONN. Here the thickness of each bundle is correlated with the correlation value between two ROIs. The color of bundles represent the sign of the correlation, red for positive and blue for negative correlation. Left angular gyrus is negatively correlated with the right inferior frontal gyrus in group two, three and four.

	Unnamed: 0	LIFGorb	LIFG	LMFG	LAntTemp	LPostTemp	LAngG	RIFGorb	RIFG	RMFG	RantTemp	RpostTemp	RangG
0	LIFGorb	0	0	0	1	0	0	0	0	0	1	1	0
1	LIFG	0	0	0	0	0	0	0	0	0	0	1	0
2	LMFG	0	0	0	0	0	0	0	1	0	0	1	0
3	LantTemp	1	0	0	0	0	0	1	0	0	0	1	0
4	LpostTemp	0	0	0	0	0	0	1	1	1	1	0	1
5	LangG	0	0	0	0	0	0	0	0	0	0	1	1
6	RIFGorb	0	0	0	1	1	0	0	0	0	1	0	0
7	RIFG	0	0	1	0	1	0	0	0	0	0	0	0
8	RMFG	0	0	0	0	1	0	0	0	0	0	0	0
9	RantTemp	1	0	0	0	1	0	1	0	0	0	0	0
10	RpostTemp	1	1	1	1	0	1	0	0	0	0	0	0
11	RangG	0	0	0	0	1	1	0	0	0	0	0	0

Fig. 3.11 Significant pairs of ROI with higher connectivity in familiarity group one than four, obtained from the one tailed-two-sample t-test with $p<0.05$, with the same sequence of ROI plotted in the figure 3.12.

	Unnamed: 0	LIFGorb	LIFG	LMFG	LAntTemp	LPostTemp	LAngG	RIFGorb	RIFG	RMFG	RantTemp	RpostTemp	RangG
0	LIFGorb	0	0	0	0	1	0	0	0	0	0	0	0
1	LIFG	0	0	0	0	1	1	0	0	0	0	0	0
2	LMFG	0	0	0	1	1	1	0	0	0	0	0	0
3	LantTemp	0	0	1	0	1	0	0	0	0	0	0	0
4	LpostTemp	1	1	1	1	0	1	0	0	0	0	0	0
5	LangG	0	1	1	0	1	0	0	0	0	0	0	0
6	RIFGorb	0	0	0	0	0	0	0	0	1	0	1	0
7	RIFG	0	0	0	0	0	0	0	0	1	0	1	0
8	RMFG	0	0	0	0	0	0	1	1	0	0	1	0
9	RantTemp	0	0	0	0	0	0	0	0	0	0	0	0
10	RpostTemp	0	0	0	0	0	0	1	1	1	0	0	1
11	RangG	0	0	0	0	0	0	0	0	0	0	1	0

Fig. 3.12 Significant pairs of ROI with higher connectivity in familiarity group four than one, obtained from the one tailed-two-sample t-test with $p<0.05$, with the same sequence of ROI plotted in the figure 3.12.

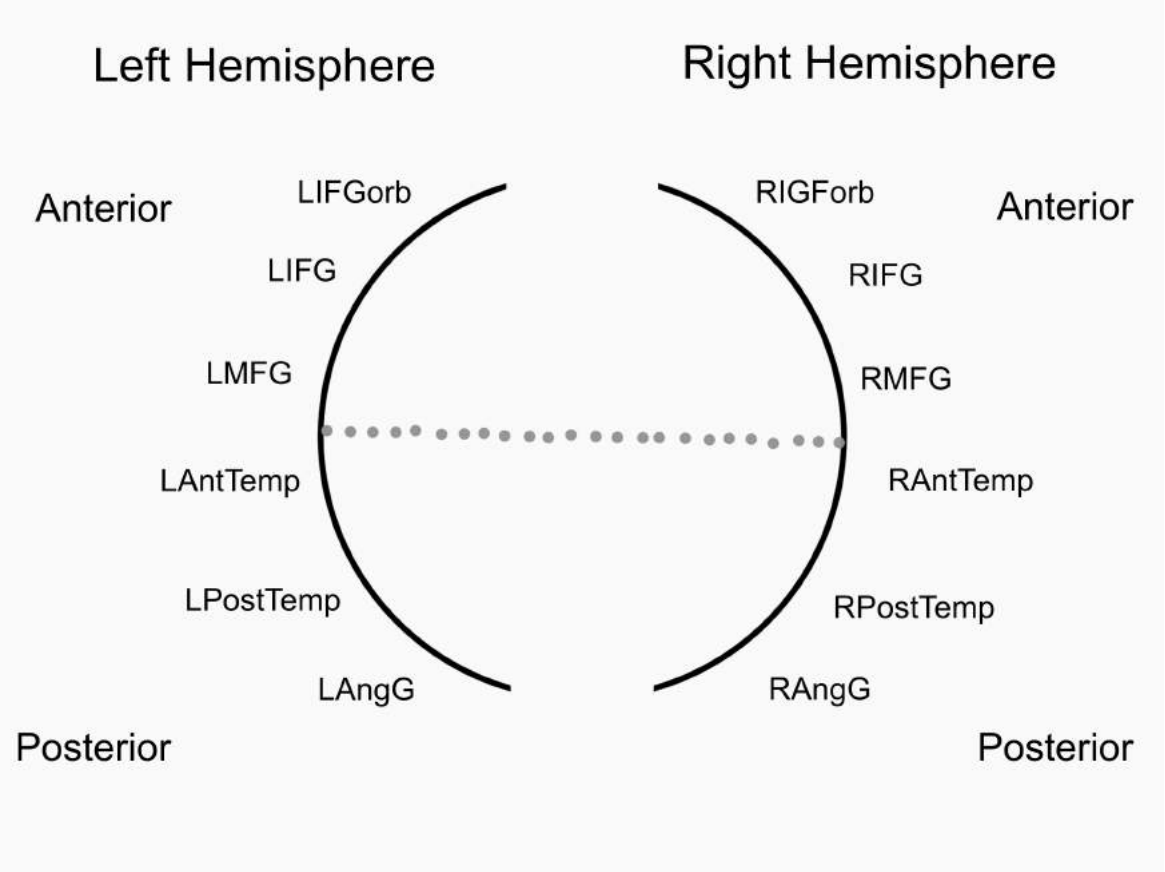

Fig. 3.13 Graphical ring for navigating through the connectivity rings generated by CONN toolbox showing functional connectivity (z-transformed correlation values) between the language regions, left and right

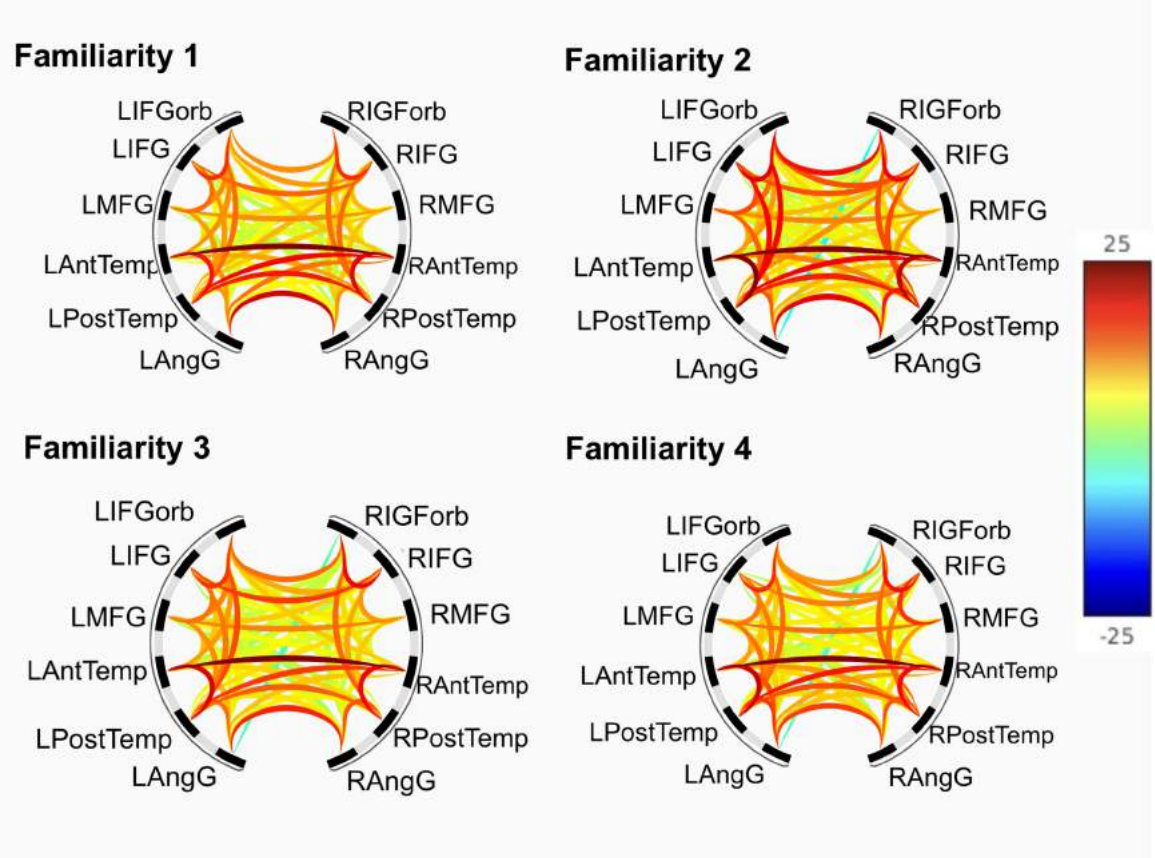

Fig. 3.14 Suprathreshold ($p<0.05$) functional connectivity ring for all the language ROIs, where the language ROIs are mentioned on the circumference and the connections between them are color-coded with the z-scored correlational values with the range from -25 to 25. The left hemisphere is represented by the upper semi-circle and the right hemisphere by the lower half of the ring.

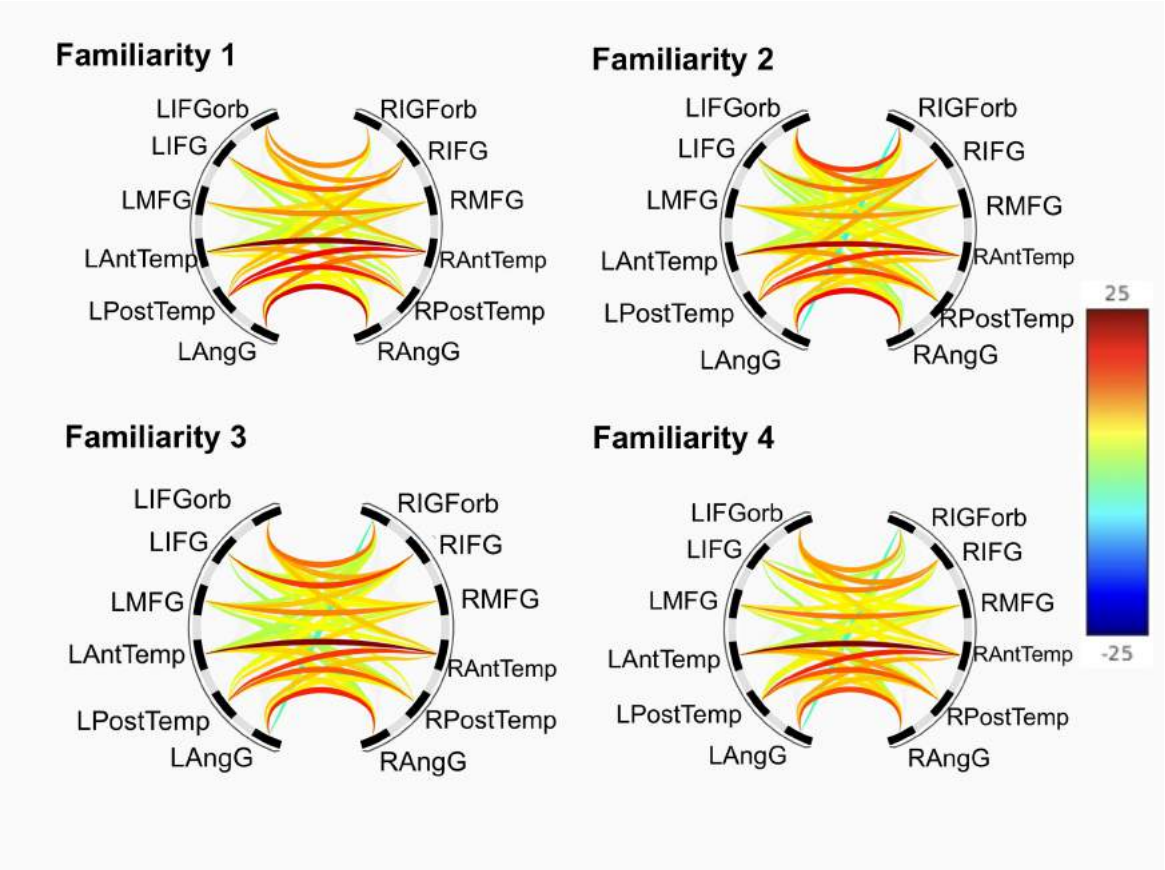

Fig. 3.15 Suprathreshold functional connectivity ring depicting only inter-hemispheric connections, where the language ROIs are mentioned on the circumference and the connections between them are color-coded with the z-scored correlational values with the range from -25 to 25. The left hemisphere is represented by the upper semi-circle and the right hemisphere by the lower half of the ring.

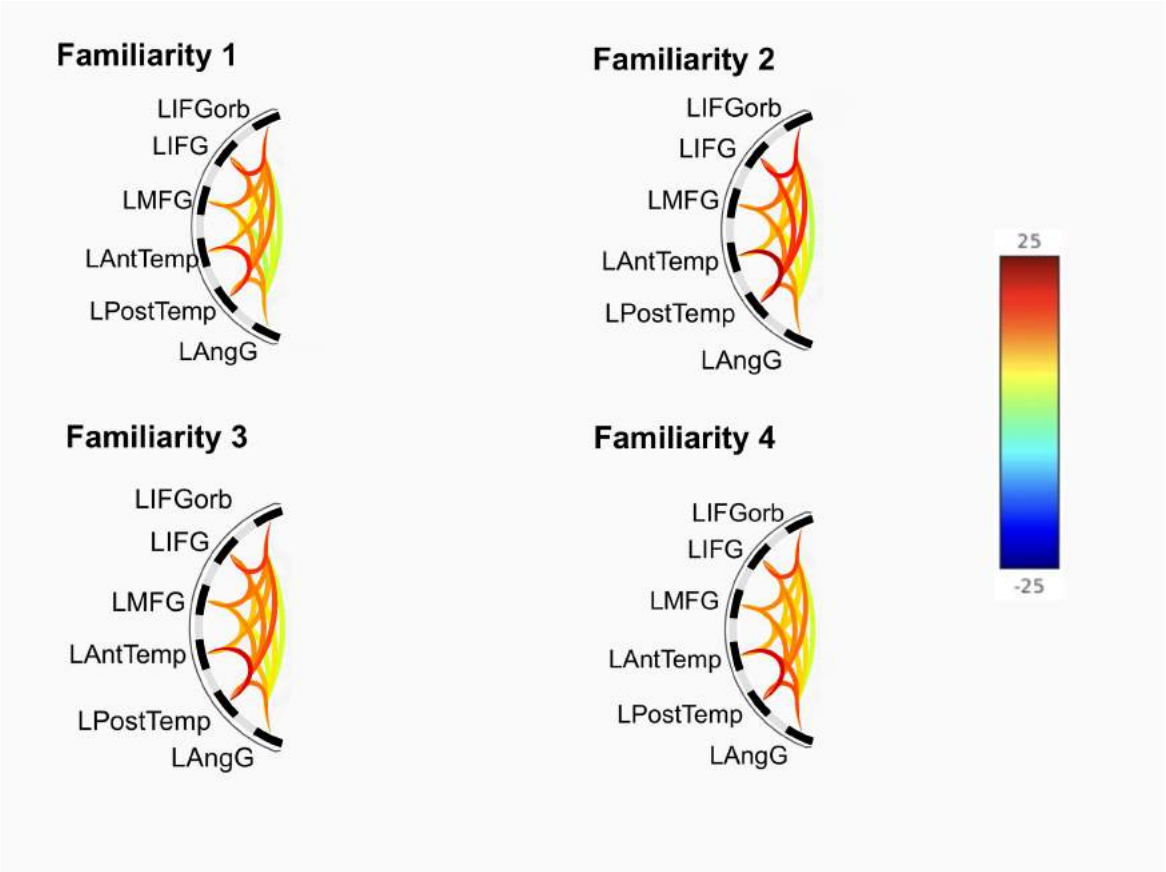

Fig. 3.16 Suprathreshold functional connectivity ring depicting only left hemispheric connections, where the language ROIs are mentioned on the circumference and the connections between them are color-coded with the z-scored correlational values with the range from -25 to 25. The left hemisphere is represented by the upper semi-circle and the right hemisphere by the lower half of the ring.

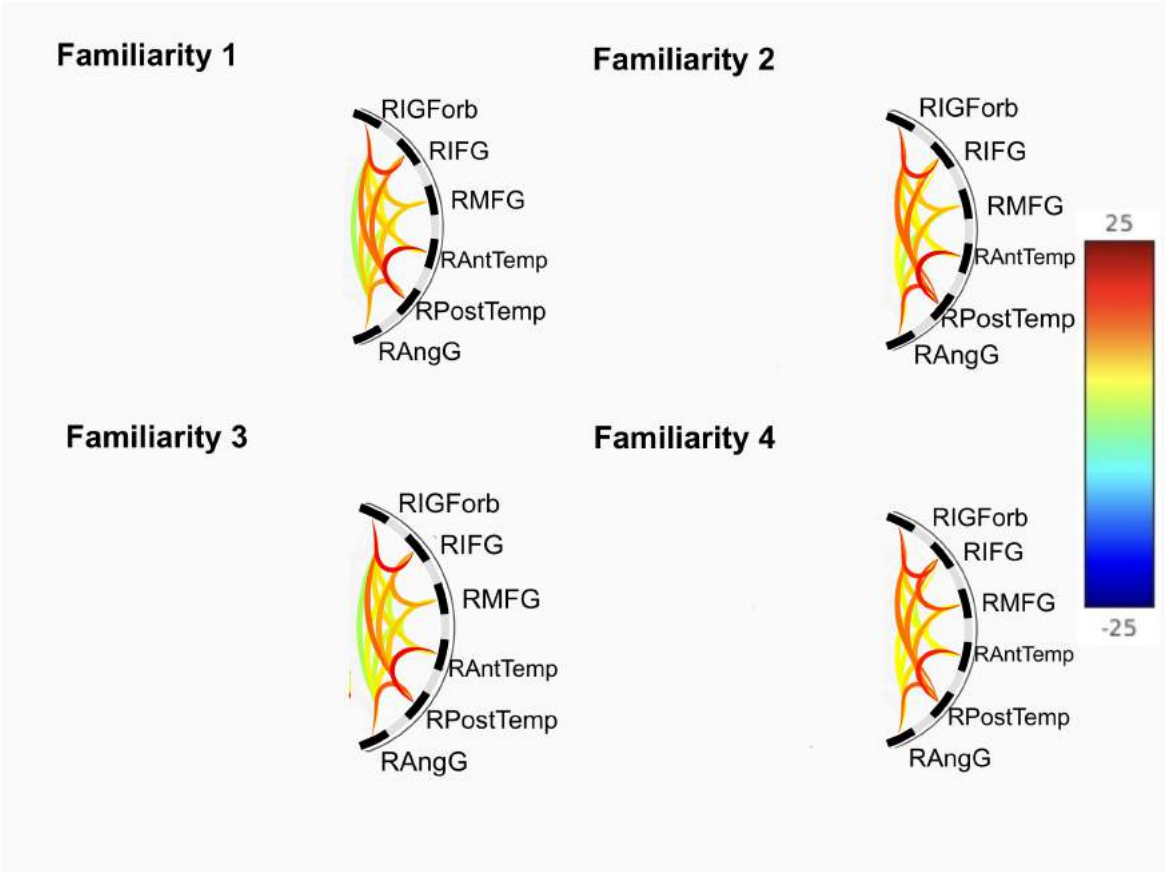

Fig. 3.17 Suprathreshold functional connectivity ring depicting only right hemispheric connections, where the language ROIs are mentioned on the circumference and the connections between them are color-coded with the z-scored correlational values with the range from -25 to 25. The left hemisphere is represented by the upper semi-circle and the right hemisphere by the lower half of the ring.

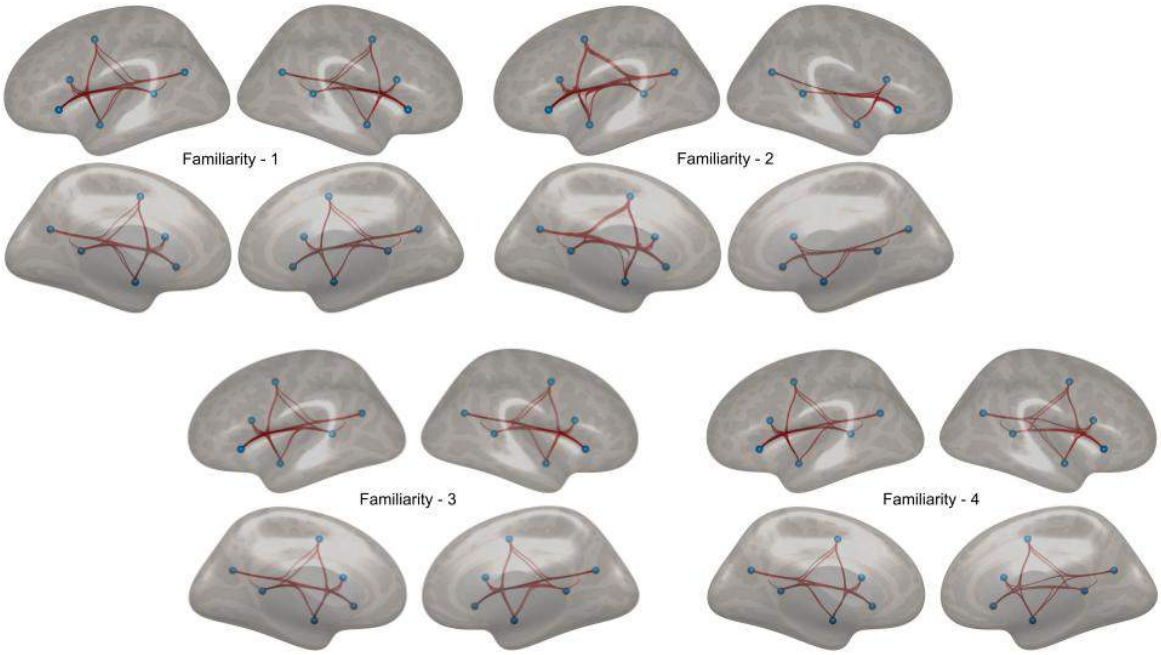

Fig. 3.18 Functional Connectivity between language ROIs rendered on the 3D brain showing left and right lateral and middle views for each group, spherical ROIs are in blue and the functional connections are represented by the opacity of the bundles, thresholded at $p<0.05$. The positive correlation value is represented by the red bundles and the negative correlation value by blue bundles

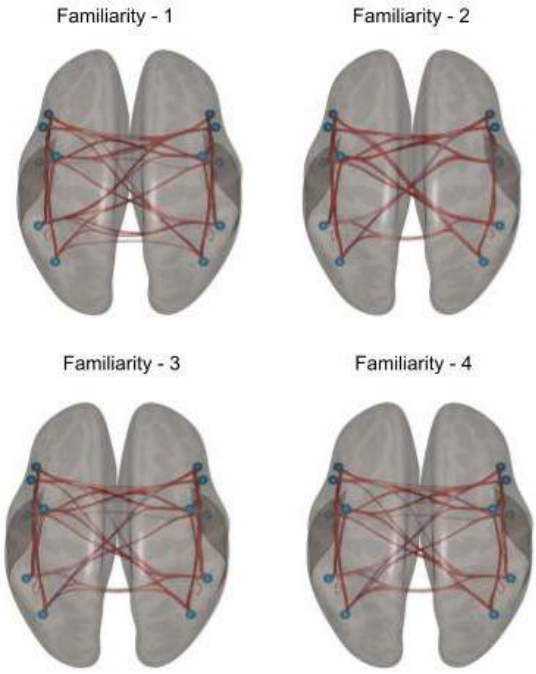

Fig. 3.19 Superior view of the functional Connectivity between language ROIs rendered on the 3D brain for each group, spherical ROIs are in blue and the functional connections are represented by the opacity of the bundles, thresholded at $p<0.05$. The positive correlation value is represented by the red bundles and the negative correlation value by blue bundles

Chapter 4

Discussion

4.1 Why do we limit the study only to language areas?

The fact that the responses elicitepd during sentence comprehension are consistent across left-hemispheric frontotemporal regions - the domain-specific language network is well known in the literature (Diachek et al., 2020). Aside from the language network, the domain-general frontoparietal, also known as the multiple-demand network, was also known to be activated during sentence processing, mainly for executive processes. On the contrary, recent studies have proven that these activations in the MD network are because of the extraneous task demands and the language-specific regions perform all the core linguistic processes. The language-specific regions maintain all the core aspects of sentence comprehension, such as inhibiting irrelevant meanings, predicting the next word, and keeping the intermediate representations active in the working memory. Hence, we reduced our regions under investigation to only to the language-specific areas defined by the ROI parcels. This reduction presumably abates the efforts to understand the higher-level processes during sentence comprehension of these smaller set of regions but simultaneously blurring the picture for the function and the connectivity with different regions, of each ROI.

Working memory load during the sentence processing has storage and integration costs, which are associated with maintaining the meaning and retrieving representations in/from the working memory, respectively. The researchers have observed a strong integration cost and a weaker storage cost in the language tasks but no reliable effects in the executive network for the surprisal effects. (Shain et al., 2021)

There is a need for further studies to track the precise locations and pathways within the language network responsible for next word prediction, storage in the working memory and the inhibition of the incorrect meaning because only do we know now is that the language network plays a significant role but how and which area exactly is, still to be answered.

4.2 Inferences from functional connectivity

On comparing the changes in the static functional connectivity of the sentence reading with the progressively increasing self-rating for the familiarity with the topic of the subject read, we found that the different patterns of ROI pairs are co-activated for distinct familiarity scores. In order to propose a general theory, we nosedived deeper into the differences between the groups with the highest and the lowest familiarity scores. As it can be seen from figure 3.11 that the sessions with the low familiarity have higher connectivity between inter-hemispheric homologues than the with high familiarity. And on the flip side, the intra-hemispheric regions show higher connectivity when compared with group one (mainly, the posterior left hemisphere has more than the right hemispheric regions). This validates the idea of higher local coherence with high familiarity, whereas there is higher cross-hemispheric talk between the left and right hemispheric regions. One can reason that while processing a cognitively loaded low familiarity paragraph, the right homologues support the left-hemispheric regions.

4.3 Something special at familiarity two?

Familiarity group two stands out in behavioural text (high variance), in t-maps (higher activations) and connectivity analysis (more increased intra-left-hemispheric connectivity). While trying to relate these divergences to the psychological state, we proposed the reason that the familiarity score of the two means that the reader is not entirely unaware of the topic but doesn't wholly apprehends it as well. They will put more effort into comprehending the passage and will be able to link the concepts somewhat more than the complete neophyte person to the topic, hence, increasing the cognitive load. The reader with high familiarity with the scientific topic will barely put effort into understanding and connecting the important conceptual links. The psychological state represented above might be the underlining rationale for the divergence; the question is still open to scrutiny.

4.4 Left Angular Gyrus - owning the "right" activity profile

Left angular gyrus had a negative percent signal change (around -0.02 %) for every group except the familiarity group two, which had a positive but minuscule percent signal change (0.002 %). It is evident that the left AngG doesn't neatly follow the left hemispheric trend of positive percent signal change during language comprehension, and its role in the core language processing tasks has been debated for a long time. AngG is structurally distant from the rest of the language network (frontotemporal) and has been implicated in a broad range of cognitive processes, including its robust response to language tasks. Literature has reported the activation of the left angular gyrus in semantic processing, executive processing, numerical cognition and some aspects of social cognition (Seghier, 2013). Its strong uncoupling with the other language regions has been shown in multiple previous studies, including the most recent one, which looked at the dynamical reconfiguration of the language network during the semantic relatedness judgement task (Chai et al., 2016). The left angular gyrus doesn't appear to be modulated by the syntactic complexity and doesn't show semantic > numerical effect. Since it appears consistently in the language comprehension tasks, its precise role in language comprehension and the integration with the multi-demand (executive) network is yet to be discovered.

4.5 Laterality of the language network

From both the higher activations in the activation maps, evaluated in part one of the study and the higher left intra-hemispheric functional connectivity evaluated in the second part of our study, it was evident that the left frontotemporal and temporoparietal regions were more involved in the language comprehension task than the right hemispheric homologues. Since Gazzaniga's pioneering work (Gu et al., 2015), the left lateralization of language processing has been studied for the past sixty years. Earlier, only the individual regions were considered left-lateralized, but recently the view shifted to the entire language network being lateralized to the left (Doron et al., 2012). The activations during the task condition mirror the distinct neural activations in both the hemispheres, probably supporting dissimilar computations (Bassett et al., 2015).

4.6 Right Homologous Regions

We found no activation in the right hemispheric regions, the percent signal change was negative indicating the active inhibition by the left hemispheric language regions and the negative BOLD response may not be mapping the neural activity one-to-one in the right regions. Also, the connectivity between the right hemispheric regions was lower than intra-left hemispheric connectivity for all the groups.

Although language processing is believed to be left-lateralized, multiple neuroimaging studies have reported right inferior frontal and temporal areas in various linguistic tasks. During the word fluency and sentence completion task in healthy subjects, the performance scores were directly correlated with the right hemispheric activation in the inferior frontal gyrus and negatively correlated with the dorsolateral prefrontal cortex activations, reinforcing the theory of right regions supporting the left-hemispheric regions (Van Ettinger-Veenstra et al., 2012). A meta-analysis on the non-literal language (Rapp et al., 2012) showed that mostly the right hemispheric regions are responsible for metaphors, metonymy, irony and idioms, jokes and some aspects of prosody - the periphery linguistic comprehension. Hence, the famously suggested inference of two computational levels of language processing, the core computations, supported by the left language areas and the peripheral computations, supported by the right homologues.

4.7 Supplementary motor areas during silent reading

We found supplementary motor areas actively participating in the perception of language processing during the task conditions in all the groups, maximum in group two. During silent reading, the visual information is transduced to auditory phonological code in the grapheme-to-phenome conversion process (GPC) by the precentral gyrus, as reported in a recent cortical electrophysiological study (Kaestner et al., 2022). The precentral gyrus is mainly responsible for the rehearsal of the speech before the utterance, but the studies have also shown that as the reading skills increase during development, there is a shift in information reliance from phonological to orthographic, and the phonological information continues to influence reading even during visual inputs. (Harm and Seidenberg, 2004) (Rastle and Brysbaert, 2006)

4.8 Limitations

While analysing the data, we encountered some setbacks in the experiment design. We aimed to look at the paragraph level changes during reading comprehension, and we chose the control/baseline to be the small fixation blocks at the beginning and the end of the paragraph. The fixation blocks were of much lesser duration than the task condition (6 and 10 seconds long compared to at least a minute long tasks). Also, the inter-sentence interval of 0.5 seconds was overridden and included in the paragraph block. Supplementary: We tried using the resting state data as the baseline but failed to do so because of the difference in the TR and hence, different temporal signal to noise ratios (TR = 2 secs for resting and TR = 0.4 secs for task runs).

Also, the parcellation used to define the ROIs was based on the activations for sentence > non-words, but the individual ROI was huge compared to the activations in each region in every subject. While averaging across the ROI, it is very well possible that we are including the voxels from both the language and executive regions, as these networks lie close to each other and have opposing activity profiles during the language comprehension task, leading to lower values (percent change and connectivity) than expected. We plan to do a subject-specific analysis to classify active voxels to combat this issue.

4.9 Conclusion and Future Directions

While processing scientific texts, there were clear differences between high and low familiarity in the brain activations and connectivity in the language-specific areas. From the activations for sentence reading, subtracted from fixations, the left-language specific regions recruited a lesser number of voxels for high familiarity than while processing a text with low familiarity. Also, it was evident from the percent signal change and t-values that the BOLD response decreases in the same ROIs with increasing familiarity. During sentence comprehension, functional connectivity between the inter-hemispheric language regions was higher in the low familiarity group. The intra-hemispheric region had higher connectivity values in the high familiarity group.

The familiarity two stood out from the linear trend, in both the activation maps with the most number of voxels and highest percent signal change, and the functional connectivity, with the most increased intra-left hemispheric connectivity. The state of being partly familiar with the context of the paragraph seems to be engaging

the language network the most. Moreover, the analysis revealed unambiguous left-lateralized effects during language processing, with the left angular gyrus, reported following the right-hemispheric activation profile, as the notable exception to the trend.

From both the activation and the functional connectivity patterns, it was prominent that the more familiar one is with the context of the reading material, the more computationally efficient is the corresponding language network - recruiting lesser voxels and residing the higher functional connectivity in the left-hemispheric language regions.

In our future analyses, we aim to look for the causal dynamics of the left and right hemispheric language regions and also how the between-network functional connectivity changes with the familiarity scores, for example between the language and the dorsal attention network, and language and the default mode network.

References

Bassett, D. S., Yang, M., Wymbs, N. F., and Grafton, S. T. (2015). Learning-induced autonomy of sensorimotor systems. *Nature neuroscience*, 18(5):744–751.

Chai, L. R., Mattar, M. G., Blank, I. A., Fedorenko, E., and Bassett, D. S. (2016). Functional Network Dynamics of the Language System. *Cerebral Cortex*, 26(11):4148–4159.

Chen, L., Wassermann, D., Abrams, D. A., Kochalka, J., Gallardo-Diez, G., and Menon, V. (2019). The visual word form area (vwfa) is part of both language and attention circuitry. *Nature Communications*, 10(1):5601.

Diachek, E., Blank, I., Siegelman, M., Affourtit, J., and Fedorenko, E. (2020). The domain-general multiple demand (md) network does not support core aspects of language comprehension: A large-scale fmri investigation. *Journal of Neuroscience*, 40(23):4536–4550.

Doron, K. W., Bassett, D. S., and Gazzaniga, M. S. (2012). Dynamic network structure of interhemispheric coordination. *Proceedings of the National Academy of Sciences*, 109(46):18661–18668.

Fedorenko, E., Hsieh, P.-J., Nieto-Castanon, A., Whitfield-Gabrieli, S., and Kanwisher, N. (2010). New method for fmri investigations of language: Defining rois functionally in individual subjects. *Journal of neurophysiology*, 104:1177–94.

Friston, K., Ashburner, J., Kiebel, S., Nichols, T., and Penny, W., editors (2007). *Statistical Parametric Mapping: The Analysis of Functional Brain Images*. Academic Press.

Frost, J. A., Binder, J. R., Springer, J. A., Hammeke, T. A., Bellgowan, P. S., Rao, S. M., and Cox, R. W. (1999). Language processing is strongly left lateralized in both sexes: Evidence from functional MRI. *Brain*, 122(2):199–208.

Glasser, M., Sotiropoulos, S., Wilson, J., Coalson, T., Fischl, B., Andersson, J., Xu, J., Jbabdi, S., Webster, M., Polimeni, J., DC, V., and Jenkinson, M. (2013a). The minimal preprocessing pipelines for the human connectome project. *NeuroImage*, 80:105.

Glasser, M. F., Sotiropoulos, S. N., Wilson, J. A., Coalson, T. S., Fischl, B., Andersson, J. L., Xu, J., Jbabdi, S., Webster, M., Polimeni, J. R., Van Essen, D. C., and Jenkinson, M. (2013b). The minimal preprocessing pipelines for the human connectome project. *NeuroImage*, 80:105–124. Mapping the Connectome.

Gu, S., Satterthwaite, T. D., Medaglia, J. D., Yang, M., Gur, R. E., Gur, R. C., and Bassett, D. S. (2015). Emergence of system roles in normative neurodevelopment. *Proceedings of the National Academy of Sciences*, 112(44):13681–13686.

Han, H. and Glenn, A. L. (2018). Evaluating methods of correcting for multiple comparisons implemented in spm12 in social neuroscience fmri studies: an example from moral psychology. *Social Neuroscience*, 13(3):257–267. PMID: 28446105.

Harm, M. W. and Seidenberg, M. S. (2004). Computing the meanings of words in reading: cooperative division of labor between visual and phonological processes. *Psychological review*, 111(3):662.

Hertrich, I., Dietrich, S., and Ackermann, H. (2020). The margins of the language network in the brain. *Frontiers in Communication*, 5.

Hsu, C.-T., Clariana, R., Schloss, B., and Li, P. (2019). Neurocognitive signatures of naturalistic reading of scientific texts: A fixation-related fmri study. *Scientific Reports*, 9(1):10678.

Jafri, M. J., Pearlson, G. D., Stevens, M., and Calhoun, V. D. (2008). A method for functional network connectivity among spatially independent resting-state components in schizophrenia. *NeuroImage*, 39(4):1666–1681.

Kaestner, E., Wu, X., Friedman, D., Dugan, P., Devinsky, O., Carlson, C., Doyle, W., Thesen, T., and Halgren, E. (2022). The Precentral Gyrus Contributions to the Early Time-Course of Grapheme-to-Phoneme Conversion. *Neurobiology of Language*, 3(1):18–45.

Li, P., Hsu, C.-T., Schloss, B., Yu, A., Ma, L., Scotto, M., Seyfried, F., and Gu, C. (2022). "the reading brain project l1 adults".

Mar, R. A., Li, J., Nguyen, A. T. P., and Ta, C. P. (2021). Memory and comprehension of narrative versus expository texts: A meta-analysis. *Psychonomic Bulletin & Review*, 28(3):732–749.

Pedregosa-Izquierdo, F. (2015). *Feature extraction and supervised learning on fMRI : from practice to theory*. Theses, Université Pierre et Marie Curie - Paris VI.

Polimeni, J. R. and Lewis, L. D. (2021). Imaging faster neural dynamics with fast fmri: A need for updated models of the hemodynamic response. *Progress in Neurobiology*, 207:102174. How high spatiotemporal resolution fMRI can advance neuroscience.

Rapp, A. M., Mutschler, D. E., and Erb, M. (2012). Where in the brain is nonliteral language? a coordinate-based meta-analysis of functional magnetic resonance imaging studies. *Neuroimage*, 63(1):600–610.

Rastle, K. and Brysbaert, M. (2006). Masked phonological priming effects in english: Are they real? do they matter? *Cognitive Psychology*, 53(2):97–145.

Seghier, M. L. (2013). The angular gyrus: Multiple functions and multiple subdivisions. *The Neuroscientist*, 19(1):43–61. PMID: 22547530.

Shain, C., Blank, I. A., Fedorenko, E., Gibson, E., and Schuler, W. (2021). Robust effects of working memory demand during naturalistic language comprehension in language-selective cortex. *bioRxiv*.

Todd, N., Moeller, S., Auerbach, E. J., Yacoub, E., Flandin, G., and Weiskopf, N. (2016). Evaluation of 2d multiband epi imaging for high-resolution, whole-brain, task-based fmri studies at 3t: Sensitivity and slice leakage artifacts. *NeuroImage*, 124:32–42.

Tripathi, K. N., Bihari, A., Tripathi, S., and Mishra, R. B. (2020). A review on brain mechanisms for language acquisition and comprehension.

Van Ettinger-Veenstra, H., Ragnehed, M., McAllister, A., Lundberg, P., and Engström, M. (2012). Right-hemispheric cortical contributions to language ability in healthy adults. *Brain and language*, 120(3):395–400.

Whitfield-Gabrieli, S. and Nieto-Castanon, A. (2012). Conn : A functional connectivity toolbox for correlated and anticorrelated brain networks. *Brain Connectivity*, 2:125–41.